The Nonphagocytic NADPH Oxidase Duox1 Mediates a Positive Feedback Loop During T Cell Receptor Signaling

Jaeyul Kwon[1,2,*], **Kristen E. Shatynski**[1], **Haiyan Chen**[1], **Stanislas Morand**[2], **Xavier de Deken**[3], **Françoise Miot**[3], **Thomas L. Leto**[2], and **Mark S. Williams**[1,*]

[1]Center for Vascular and Inflammatory Diseases, Department of Microbiology and Immunology, University of Maryland School of Medicine, 800 West Baltimore Street, Baltimore, MD 21201, USA.

[2]Laboratory of Host Defenses, National Institute of Allergy and Infectious Diseases, National Institutes of Health, 12441 Parklawn Drive, Rockville, MD 20852, USA.

[3]Institut de Recherche Interdisciplinaire en Biologie Humaine et Moléculaire, Université Libre de Bruxelles, Campus Erasme, 1070 Brussels, Belgium.

Abstract

Production of reactive oxygen species, often by NADPH (reduced form of nicotinamide adenine dinucleotide phosphate) oxidases, plays a role in the signaling responses of cells to many receptor stimuli. Here, we describe the function of the calcium-dependent, nonphagocytic NADPH oxidase Duox1 in primary human CD4$^+$ T cells and cultured T cell lines. Duox1 bound to inositol 1,4,5-trisphosphate receptor 1 and was required for early T cell receptor (TCR)–stimulated production of hydrogen peroxide (H_2O_2) through a pathway that was dependent on TCR-proximal kinases. Transient or stable knockdown of Duox1 inhibited TCR signaling, especially phosphorylation of tyrosine-319 of ζ chain–associated protein kinase of 70 kilodaltons (ZAP-70), store-operated entry of calcium ions (Ca^{2+}), and activation of extracellular signal–regulated kinase. The production of cytokines was also inhibited by knockdown of Duox1. Duox1-mediated inactivation of Src homology 2 domain–containing protein tyrosine phosphatase 2 promoted the phosphorylation of ZAP-70 and its association with the Src family tyrosine kinase Lck and the CD3ζ chain of the TCR complex. Thus, we suggest that activation of Duox1, downstream of proximal TCR signals, generates H_2O_2 that acts in a positive feedback loop to enhance and sustain further TCR signaling.

INTRODUCTION

Receptor stimulation by multiple mediators, such as those for platelet-derived growth factor (1), insulin (2), or angiotensin II (3), induces the production in cells of reactive oxygen species (ROS), which control their biological functions. These ROS act as obligate second messengers, regulating protein kinase activation, gene expression, and proliferative responses. Many studies

in T cells have used exposure to exogenous oxidants, such as hydrogen peroxide (H_2O_2), to mimic or enhance signaling through the T cell receptor (TCR) (4–6). Studies have shown that TCR-induced signaling is regulated by receptor-mediated production of ROS (7), although the sources of ROS and their mechanisms of action remain unclear.

TCR signaling involves a complex array of protein kinases, phosphatases, phospholipases, and adaptor proteins (8). Engagement of the TCR with antigen induces the activation of the Src family tyrosine kinase Lck, which phosphorylates immunoreceptor tyrosine-based activation motifs (ITAMs) on the ζ chain homodimers and CD3 chains of the TCR complex. The dually phosphorylated ITAMs create binding sites for the Src homology 2 (SH2) domains of the Syk family tyrosine kinase, ζ chain–associated protein kinase of 70 kD (ZAP-70), which in combination with Lck phosphorylates key early mediators of TCR signaling, including the adaptor proteins linker of activated T cells (LAT) and SH2 domain–containing leukocyte phosphoprotein of 76 kD (SLP-76). Inhibition of these proximal signals can occur at several levels. For example, C-terminal Src kinase (Csk), which is recruited to the membrane by the adaptor protein Csk-binding protein (Cbp, also known as PAG), phosphorylates Lck at its inhibitory site, Tyr[505] (Y505) (9). Alternatively, dephosphorylation of Tyr[394] (Y394) in the activation loop of Lck by the protein tyrosine phosphatase (PTP) CD45 is proposed to inhibit proximal TCR signals (10). Similarly, other PTPs including SH2 domain–containing PTP–2 (SHP-2) (11) and SHP-1 (12,13) are thought to inhibit early TCR signaling.

In terms of downstream TCR effector signals, once the appropriate tyrosines are phosphorylated, LAT serves as a scaffold to recruit the adaptor proteins Grb2 and Gads, as well as phospholipase C–γ1(PLC-γ1) (14). Gads links with SLP-76 and brings it in proximity to LAT (15), controlling cytoskeletal changes and adhesion, whereas recruitment of Grb2 leads to activation of the Ras–mitogen-activated protein kinase (MAPK) pathway. The activity of PLC-γ1 induces increases in the concentration of cytoplasmic calcium ions (Ca^{2+}) through the production of inositol 1,4,5-trisphosphate (IP_3), which, upon binding to IP_3 receptor 1 (IP_3R1), releases Ca^{2+} from intracellular stores and activates subsequent capacitive Ca^{2+} entry through plasma membrane channels (16). These signals lead to the activation of transcription factors such as the Ca^{2+}-dependent nuclear factor of activated T cells (NFAT) and the MAPK-mediated activating protein–1 (AP-1), which initiate the expression of important regulatory genes that control cellular proliferation, differentiation, and cell survival, including interleukin-2 (IL-2) (17).

Some studies have focused on mitochondria as a source of early TCR-stimulated ROS. One report described impairment of calcium-dependent production of ROS in T cells from mice lacking expression of the genes encoding the BH3 Bcl-2 family members Bax and Bak (18), whereas another report showed that inhibitors of mitochondrial function or deletion of mitochondrial DNA inhibited TCR-induced generation of ROS in a model of activation-induced cell death (19). These data are consistent with other findings that link mitochondrial metabolic activity with the generation of ROS in activated T cells (20). Other studies, however, point to potential roles of nonmitochondrial sources of ROS in activated lymphocytes, including NADPH (reduced form of nicotinamide adenine dinucleotide phosphate) oxidases (21) and lipoxygenases (22). Investigation of the potential sources of ROS in many cell types has also identified the phagocyte-type NADPH oxidase and a family of homologs of the catalytic subunit of the oxidase (Nox and Duox proteins) that are found in nonphagocytic cells (23). Whereas the activation of oxidases in the respiratory burst of phagocytes leads to the generation of increased amounts of the superoxide anion, in nonphagocytic cells the oxidases produce less ROS, which are not cytotoxic, but regulatory. Thus, receptor signaling induces the generation of ROS from a family of NADPH oxidases that modulate cellular signaling and function.

The roles of ROS and NADPH oxidases in the regulation of T cell function are not clear and may involve several oxidases. We previously demonstrated that T cells have functional phagocyte-type NADPH oxidase (Nox2) (21). Compared to T cells from wild-type mice, T cells from *Nox2*-deficient mice exhibit defective production of H_2O_2, enhanced activation of extracellular signal–regulated kinase (ERK), and a relative increase in the amounts of secreted T helper 1 (T_H1)–type cytokines. Thus, mature T cells have a functional phagocyte-type NADPH oxidase that appears to inhibit some elements of TCR signaling; however, an early phase of H_2O_2 generation in T cells is independent of Nox2. This generation of H_2O_2 occurs within 2 to 4 min of TCR stimulation and is consistent with the kinetics of early TCR signaling and TCR-induced oxidation of PTPs, as described previously (24). Thus, the goal of the current study was to determine the sources of this early TCR-stimulated H_2O_2 and its role in TCR signaling.

Here, we demonstrate that Duox1, a Ca^{2+}-dependent nonphagocytic NADPH oxidase, is responsible for early TCR-stimulated generation of H_2O_2. Activation of Duox1 was dependent on early tyrosine kinase signaling, PLC-γ1, and the release of Ca^{2+} from the endoplasmic reticulum (ER). Knockdown of Duox1 in primary human CD4+ T cells and Jurkat cells (a human CD4+ T cell leukemia cell line) selectively inhibited the generation of H_2O_2 and the phosphorylation of proximal signaling molecules, suggesting a positive role for Duox1 in TCR signal transduction. Specifically, phosphorylation of Tyr^{319} (Y319) in ZAP-70 and activation of ERK were inhibited by knockdown of Duox1, and these effects were reversed upon reconstitution of cells with Duox1. Duox1 was coimmunoprecipitated with IP$_3$R1, and knockdown of Duox1 inhibited store-operated influx of Ca^{2+}, suggesting a role for Duox1-derived H_2O_2 in the regulation of Ca^{2+} flux. Consistent with our previous studies (24), TCR stimulation induced the oxidation of the PTP SHP-2, which was diminished in T cells with stable knockdown of Duox1. These data support a model in which Duox1-mediated oxidation of SHP-2 enhances proximal TCR signaling through regulation of the phosphorylation and activation of ZAP-70. Thus, the results suggest that Duox1-mediated production of H_2O_2, which is dependent on proximal TCR signal pathways, is a key mediator of TCR signaling that acts in a positive feedback loop to promote proximal and downstream TCR signal transduction.

RESULTS

Signals that regulate the early generation of ROS

In Jurkat cells, cross-linking (stimulation) of the TCR complex with antibody against CD3 (OKT3) induced the generation of ROS, as measured by the increased fluorescence of the oxidation-sensitive dye dichlorodihydrofluorescein diacetate (DCFDA) within 2 to 4 min of stimulation, which returned to baseline after ~15 min (Fig. 1A) (25). Our previous data in T cell blasts suggested that this early phase of ROS generation is independent of the phagocyte NADPH oxidase (Nox2) (21), which only affected a later phase (30 min) of DCFDA oxidation; however, our current studies suggested potential roles for another NADPH oxidase in early TCR-stimulated generation of ROS. All subsequent experiments monitored this early phase of ROS generation by measuring the amount of oxidized DCFDA present 10 or 15 min after TCR cross-linking (26). Some NADPH oxidases, such as Nox1, Nox2, and Nox3, are dependent on the small guanosine triphosphatase (GTPase) Rac1, whereas others, such as Nox4, Nox5, Duox1, and Duox2, may not require Rac1 (27–29). Expression of a dominant-negative (DN) Rac1 (N17Rac1) did not inhibit early TCR-induced oxidation of DCFDA (fig. S1A). Oxidation of DCFDA was sensitive to the general flavin electron transfer inhibitor diphenylene iodonium (DPI) (fig. S1B). Thus, these data are consistent with a Rac-independent NADPH oxidase as a potential source of ROS early after stimulation of the TCR.

To further delineate biochemically the signaling steps required for the early TCR-induced generation of ROS, we manipulated early TCR signals with pharmacologic and molecular

tools. Consistent with previous studies (19), Jurkat cell lines deficient in Lck or ZAP-70 did not exhibit TCR-induced generation of ROS (Fig. 1B). The TCR-induced increase in the concentration of intracellular Ca^{2+} is controlled through PLC-γ1–mediated production of IP_3 and its binding to IP_3R1. Jurkat cells deficient in PLC-γ1 (J.gamma1) (30) or IP_3R1 (IP_3R1-deficient) (31) generated substantially less ROS upon TCR stimulation than did control cells (Fig. 1C). Reconstitution of J.gamma1 cells with wild-type PLC-γ1 (to generate J.gamma1.WT cells) partially restored the oxidation of DCFDA in response to TCR stimulation. Furthermore, transfection of Jurkat cells with a plasmid encoding a DN mutant (Y783F) of PLC-γ1(32) inhibited the generation of ROS (Fig. 1D). Consistent with the importance of PLC-γ1 in this process, stable Jurkat cell clones that had mutations in the adaptor protein SLP-76 that prevented SLP-76 from associating with or activating PLC-γ1(Y3Fand ΔGads, respectively) (33) showed a marked decrease in the extent of TCR-induced generation of ROS relative to that of cells transfected with a plasmid encoding either a full-length or a variant SLP-76 with a mutation in the SH2 domain that prevents its association with adhesion- and degranulation-promoting adaptor protein (ADAP) (mSH2) (Fig. 1E). Furthermore, chelating intra-cellular Ca^{2+} with BAPTA [1,2-bis(o-aminophenoxy) ethane-N, N, N', N'-tetraacetic acid] inhibited the early generation of ROS in Jurkat cells (Fig. 1F). Together, these data are suggestive of a role for intracellular Ca^{2+} in controlling the generation of ROS; however, extracellular Ca^{2+} was not required for the oxidation of DCFDA, as determined in the presence of EGTA or upon stimulation of cells in Ca^{2+}-free buffer (Fig. 1F). Thus, mechanisms that control TCR-induced increases in the release of Ca^{2+} from intracellular stores are required for the early generation of ROS, and the data are consistent with a role for a Ca^{2+}-dependent NADPH oxidase that is DPI-sensitive but that does not require Rac1.

Ca^{2+} flux alone was not sufficient for the generation of ROS because exposure to thapsigargin (Fig. 2A) or ionomycin (Fig. 2B), which increases the concentration of intracellular Ca^{2+}, in the absence of TCR stimulation did not induce the oxidation of DCFDA. Co-incubation of cells with either drug during TCR stimulation did not markedly augment the extent of DCFDA oxidation when compared with that in TCR-stimulated cells in the absence of drug. The addition of ionomycin or thapsigargin to PLC-γ1–deficient Jurkat cells restored TCR-induced oxidation of DCFDA to an extent similar to that observed in cells in which PLC-γ1 was restored (Fig. 2, A and B). Thus, these data suggest that TCR-stimulated release of Ca^{2+} from intracellular stores is necessary, but not sufficient, for the early generation of ROS, and that other elements of TCR signaling are required.

Expression of Duox1 messenger RNA and protein in human T cells

Given that the TCR-dependent generation of ROS was Ca^{2+}-dependent, Rac1-independent, and sensitive to DPI, we considered Duox1 and Duox2 as potential sources of ROS. Reverse transcription polymerase chain reaction (RT-PCR) analysis revealed the presence of messenger RNAs (mRNAs) for each of these oxidases in Jurkat cells and primary human $CD4^+$ T cell blasts, which was confirmed by cloning and sequencing of the PCR products (fig. S2, A and B). Duox1 and Duox2 proteins were detected in Jurkat cells by Western blotting analysis (Fig. 2C). When examining the mobility of Duox1 protein by SDS–polyacrylamide gel electrophoresis (SDS-PAGE), we found that TCR stimulation caused a shift in the mobility of Duox1 that was insensitive to dithiothreitol (DTT) (Fig. 2C). This occurred within 5 min of TCR stimulation and was reversed within 60 min, suggesting a post-translational modification, such as phosphorylation, during Duox1 activation. The kinetics of the mobility shift in Duox1 paralleled a similar shift in Lck, which is thought to be due to phosphorylation of a serine residue (25). The mobility of Duox2 was affected neither by TCR stimulation nor by DTT. Further analysis showed that stimulation of Jurkat cells with the phorbol ester PMA (phorbol 12-myristate 13-acetate) also induced a mobility shift in Duox1 protein (Fig. 2D). These data are suggestive of the phosphorylation of Duox1 upon TCR stimulation. Western blotting

analysis showed that immunoprecipitated Duox1 was detected with either a monoclonal antibody against phosphoserine (pSer) residues or an antibody against substrates of protein kinase C (PKC) that recognizes a pSer in the consensus sequence (R/K)XS(Hyd)(R/K) (Fig. 2E). These data are consistent with earlier results (Fig. 2, A and B), which suggest that a TCR-induced signal in addition to Ca^{2+} flux is required for the activation of Duox1. In addition, the data agree with a previous report that Nox5, one of the Ca^{2+}-dependent members of the Nox family, undergoes serine phosphorylation, which enhances its responsiveness to lower concentrations of Ca^{2+} (34).

Effects of suppressed expression of *Duox1* on TCR signaling in Jurkat cells

Commercially available small interfering RNAs (siRNAs) were analyzed for their ability to inhibit the expression of *Duox1* or *Duox2* transcripts (fig. S2C) in Jurkat cells, which were transfected with nontargeting (NT) siRNAs as a control. Duox1-specific, but not Duox2-specific, siRNAs substantially inhibited early (10 min) oxidation of DCFDA after TCR stimulation (fig. S2D). Thus, these data suggest that Duox1 was responsible for early TCR-stimulated generation of ROS. To further examine the role of Duox1 in TCR signaling, we isolated stable clones of Jurkat cells after transfection with either a plasmid encoding short hairpin RNA (shRNA) specific for Duox1 or an NT vector (NT cells). The abundance of Duox1 protein was substantially reduced in the Duox1-targeted cell clone (Fig. 3A), whereas the abundance of Duox2 protein was unaffected. In addition, the abundance of the phagocytic oxidase Nox2 was also unaffected by knockdown of Duox1. TCR-stimulated early oxidation of DCFDA, which occurred within 10 or 15 min in NT cells, was almost completely absent in the Duox1-targeted cells (Fig. 3B). At longer time points, however, there was still measurable generation of ROS, although it was substantially decreased compared to that in the NT cells (Fig. 3B). Together, these data are consistent with the presence of functional Duox1 in T cells and its role in early TCR-stimulated generation of ROS.

In experiments with the stable Duox1-knockdown clone of Jurkat cells, we investigated the effects of early generation of H_2O_2 on TCR signaling (Fig. 3, C to E). Downstream functional consequences of the signaling changes caused by knockdown of Duox1 were measured with luciferase-based reporter constructs for the transcription factors AP-1 and NFAT. TCR-induced activation of both reporter constructs was substantially inhibited in the Duox1-knockdown cells compared to that in the NT cells (Fig. 3C). Thus, Duox1 was also required for optimal TCR-induced activation of AP-1 and NFAT, which suggests that Duox1 is needed for the activation of ERK, which regulates AP-1 activation, and for the increase of intracellular Ca^{2+} concentrations, which is required for the nuclear translocation of NFAT.

Knockdown of Duox1 inhibited the TCR-induced phosphorylation of ERK1 and ERK2 and that of the Syk family kinase ZAP-70 at Tyr[319],suggesting that Duox1-dependent generation of H_2O_2 plays a positive role in their activation (Fig. 3D). Phosphorylation of Tyr[319] in ZAP-70 is thought to be catalyzed by Lck or Abl (35) and is critical for the activation of ZAP-70 and of downstream signaling pathways, including the ERK pathway (36). However, phosphorylation of the inhibitory residue Tyr[505] in Lck was markedly diminished by knockdown of Duox1, whereas phosphorylation of the positive regulatory site Tyr[394] was not substantially affected (Fig. 3E). Together, these results suggest that Duox1-derived H_2O_2 may inhibit the activity of Lck by augmenting the extent of phosphorylation of Tyr[505].Furthermore, inhibition of the kinase activity of ZAP-70 did not appear to be a result of the decreased activation of Lck.

To validate the effects of knockdown of Duox1 on proximal TCR signaling in Jurkat cells, we transfected Duox1-knockdown cells with a plasmid encoding Duox1. Reconstitution of Duox1-knockdown cells with Duox1 reversed the phenotype, leading to the increased phosphorylation of ERK1 and ERK2, Tyr[319] of ZAP-70, and Tyr[505] of Lck (Fig. 4A). Consistent with these

observations, transfection of Jurkat cells with plasmid encoding Duox1 also augmented TCR-stimulated phosphorylation of ERK1, ERK2, and Tyr^{319} of ZAP-70 compared to that in control, untransfected cells (Fig. 4B). Conversely, transfection with plasmid encoding Duox2 did not augment, and even slightly inhibited, the activation of ERK (Fig. 4C).

Involvement of Duox1 in TCR-mediated Ca^{2+} signaling

We assessed the effects of Duox1 on intracellular Ca^{2+} mobilization because Ca^{2+} release from intracellular stores is necessary for Duox1-dependent early generation of H_2O_2, and knockdown of Duox1 inhibited TCR-induced activation of NFAT. In the context of TCR stimulation, knockdown of Duox1 strongly inhibited sustained increases in intracellular Ca^{2+} in the presence of extracellular Ca^{2+}, which was driven mainly by Ca^{2+} influx from extracellular sources (Fig. 5A). Decreased sustained intracellular Ca^{2+} concentrations were also observed in the presence of ionomycin, although the effect was milder. These strong inhibitory effects of knockdown of Duox1 were not observed in the absence of extracellular Ca^{2+}, further suggesting that upon TCR stimulation, Duox1-mediated generation of H_2O_2 stimulates the entry of Ca^{2+} through store-operated Ca^{2+} channels. Thus, these data suggest that Duox1-dependent generation of H_2O_2 is important for the Ca^{2+}-dependent immune response. Further support of the involvement of Duox1 in intracellular Ca^{2+} signaling was found by coimmunoprecipitation of IP_3R1 with Duox1 in Jurkat cells (Fig. 5B). In human embryonic kidney (HEK) 293 cells stably expressing either Duox1 or Duox2, IP_3R1 was found only in samples immunoprecipitated with an antibody against Duox1 and was not detected in samples associated with Duox2 (Fig. 5C), even though both proteins were highly abundant. Thapsigargin did not change the association between Duox1 and IP_3R1. Thus, the data further support a role for Duox1 in regulating proximal TCR signaling, especially its interaction with pathways of Ca^{2+} signaling.

Effect of knockdown of Duox1 on TCR signaling in CD4^{+} T cell blasts

Transient transfection of primary human CD4^{+} T cell blasts with the Duox1-specific siRNA, which showed the same effects that we observed in Jurkat cells, resulted in the decreased abundance of Duox1 protein, with little effect on the abundance of Duox2 protein (Fig. 6A). TCR-stimulated oxidation of DCFDA was also inhibited by the Duox1-targeting siRNA (Fig. 6B). Thus, these data support a role for Duox1 in early TCR-stimulated generation of ROS in primary T cells as well as in the Jurkat cell line. We compared TCR-induced tyrosine phosphorylation in activated human CD4^{+} T cells that had been transfected with NT siRNA or Duox1-specific siRNA (Fig. 6C). Western blotting analysis of whole-cell lysates showed that the extent of tyrosine phosphorylation of Lck, ZAP-70, TCRζ, and the adaptor molecule LAT was substantially decreased in Duox1-knockdown cells compared to that in control cells.

We also assessed the effects of knockdown of Duox1 on the activation of specific signaling molecules. Knockdown of Duox1 caused a substantial decrease in the extent of TCR-stimulated phosphorylation of Tyr^{319} of ZAP-70 and of Tyr^{783} of PLC-γ1 (Fig. 6D). To examine the functional relevance of Duox1-derived H_2O_2 in the T cell blasts, we measured TCR-induced production of cytokines. Our previous study showed that *Nox2*-deficient murine CD4^{+} T cells had a T_H1-skewed cytokine profile (21). In contrast, knockdown of Duox1 led to a general decrease in the amount of secreted cytokines without an obvious skewing to a T_H1- or T_H2-type profile. TCR-induced secretion of IL-4, IL-10, and interferon-γ (IFN-γ) by Duox1-knockdown cells was diminished by ~40% compared to that of control cells, whereas the secretion of other cytokines, such as IL-8 and RANTES, was unaffected (Fig. 6E).

Consistent with the effects of knockdown of Duox1 in Jurkat cells, knockdown of Duox1 in CD4^{+} T cell blasts led to the diminished phosphorylation of ERK compared to that in control CD4^{+} T cells (Fig. 7A). Our previous data suggested that the phosphorylation of the guanine

nucleotide exchange factor Vav1 and the SLP-76–associated adaptor protein ADAP was regulated by TCR-induced early generation of ROS (24). Indeed, knockdown of Duox1 inhibited the phosphorylation of Tyr[174] of Vav1, a key step for its activation (Fig. 7A) (37). The adaptor protein Gads recruits ADAP to LAT through SLP-76, whereas Grb2 is another critical adaptor that recruits proteins to LAT. To see the effects of knockdown of Duox1 on specific TCR-proximal phosphoproteins associated with these adaptors, we serially immunoprecipitated Gads and Grb2 from human T cells transfected with NT siRNA or Duox1-specific siRNA. Knockdown of Duox1 decreased the extent of TCR-induced phosphorylation of ADAP associated with immunoprecipitated Gads (Fig. 7B). More tyrosine-phosphorylated proteins were associated with Grb2 than with Gads (Fig. 7B), and knockdown of Duox1 markedly inhibited the extent of tyrosine phosphorylation of TCR-proximal signaling molecules, such as PLC-γ1, Lck, and LAT, which were coimmunoprecipitated with Grb2 or Gads (Fig. 7, B and C).

Thus, in primary T cell blasts, Duox1 appears to promote proximal TCR signaling, especially the phosphorylation of ZAP-70, PLC-γ1, Vav1, and ADAP, as well as the activation of ERK1 and ERK2. The Grb2-associated adaptor protein Gab2 is recruited to TCR-proximal signaling complexes through interactions with Grb2 and Gads in Jurkat cells (38). Our data showed that in human T blasts, most of Gab2 was associated with Grb2 in serial immunoprecipitations with antibodies against Gads and then Grb2 (Fig. 7B). Knockdown of Duox1 decreased the extent of phosphorylation of Gab2 and diminished its association with SHP-2 in the Grb2 immunoprecipitates (Fig. 7C).

SHP-2 associates with Gab2 and inhibits proximal TCR signaling (11). Consistent with these findings, we found that TCR stimulation increased the association between SHP-2 and Gab2, and knockdown of Duox1 abrogated the TCR-induced increase in their association in primary CD4^{+} T cell blasts (Fig. 8A). Similarly, transfection of cells with a plasmid encoding an inactive mutant of SHP-2 [SHP-2 (C/S)], which mimics an increased pool of SHP-2 inactivated by Duox1-derived H_2O_2, increased the association of SHP-2 with Gab2, suggesting that inactivation of SHP-2 affects its association with the TCR-proximal signaling complex (Fig. 8B). The interaction between Gab2 and SHP-2 is proposed to bring SHP-2 in proximity to the plasma membrane and into the proximal TCR signaling complex (38). Our previous study demonstrated that TCR-mediated early generation of ROS induced the inactivation of SHP-2 through the oxidation of its active-site cysteine (24). Thus, we focused on the potential regulation of SHP-2 by Duox1. The oxidation of the active-site cysteine residue of SHP-2 was analyzed with an antibody (oxPTP) that recognizes the sulfonic acid form of cysteine on the active-site signature motif of a PTP (39). Because the adaptor Gab2 is expected to bring SHP-2 to the membrane where the NADPH oxidase resides, we analyzed the oxidation state of SHP-2 in cytosolic and membrane fractions (Fig. 8C). TCR stimulation increased the extent of oxidation of the active-site cysteine in SHP-2, but mainly in the membrane fraction, and this was inhibited in the Duox1-knockdown cells (Fig. 8C). Thus, the data suggest that Duox1-derived H_2O_2 oxidizes the active-site cysteine of SHP-2. Furthermore, these results also suggest that the oxidation of SHP-2 occurs primarily near the plasma membrane, potentially in association with Gab2. The observations in Duox1-knockdown cells are consistent with a model in which SHP-2 is more active and efficiently dephosphorylates target substrates in the absence of H_2O_2-mediated inactivation. Such targets would include binding sites on Gab2 for the SH2 domains of SHP-2, which is supported by the decreased association of SHP-2 with Grb2 (Fig. 7C) and Gab2 (Fig. 8A). Furthermore, the opposite effect was observed in cells transfected with plasmid encoding the inactive SHP-2 mutant, SHP-2 (C/S) (Fig. 8B).

Because of previous studies that describe Gab2-mediated inhibitory effects on both ZAP-70 and TCRζ, we focused on how Duox1-mediated oxidation of SHP-2 regulated the potential effects of SHP-2 on ZAP-70. Phosphorylated Tyr[319] destabilizes the autoinhibitory interface

of ZAP-70 and stabilizes its active state (35,40). Tyr^{319} also serves as an adaptor site for the SH2 domain of Lck or PLC-γ1 (36,41), which may bring critical signaling molecules together to augment signal intensity. We transfected cells with a plasmid encoding SHP-2 (C/S) to increase the amount of inactive SHP-2, and other cells with plasmid encoding wild-type SHP-2 to increase the pool of active SHP-2. The TCR-stimulated association of ZAP-70 with TCRζ (Fig. 9A) and Lck (Fig. 9B) was enhanced in the presence of SHP-2 (C/S), as was phosphorylation of TCRζ in these complexes (Fig. 9C), which suggested that active SHP-2 inhibited the formation of a ZAP-70–Lck–TCRζ complex. Consistent with a regulatory role for SHP-2 in this complex, SHP-2 was found in Lck immunoprecipitates, and the presence of SHP-2 (C/S) increased the amount of SHP-2 associated with Lck (Fig. 9C). Knockdown of SHP-2 with specific siRNA enhanced the association between ZAP-70 and Lck in human $CD4^+$ T cells (Fig. 9D), further supporting a role for SHP-2 in this proximal signaling complex. In contrast, knockdown of Duox1 markedly diminished the TCR-stimulated association between ZAP-70 and Lck (Fig. 9E), whereas the increased abundance of Duox1 in transfected wild-type Jurkat cells augmented interactions between ZAP-70 and Lck (Fig. 9F). Thus, these data suggest that Duox1-derived H_2O_2, through the oxidative inactivation of SHP-2, enhances the activation of ZAP-70 and the phosphorylation of its substrates.

DISCUSSION

Intentional production of ROS, which function as requisite second messengers during signaling, occurs in a number of cell types in response to various stimuli. Decades ago, studies in T cells showed that exposure of cells to oxidizing agents such as pervanadate or H_2O_2 induced or enhanced the activation of proximal TCR signaling and T cell activation (4–6). Here, we demonstrated in T cells that the nonphagocytic NADPH oxidase Duox1 produced intracellular H_2O_2 upon TCR stimulation, which served in a positive feedback loop to enhance proximal TCR signaling. Duox1-derived generation of H_2O_2 in T cells was dependent on the presence of an intact TCR signaling pathway leading to the mobilization of intracellular Ca^{2+}, including PLC-γ1 and IP_3R1, because Duox1 is thought to be directly responsive to Ca^{2+} (42). The release of Ca^{2+} from intracellular stores was necessary for Duox1-dependent generation of ROS, whereas inhibition of the influx of extracellular Ca^{2+} did not lessen the production of ROS; however, an increase in the concentration of intracellular Ca^{2+} was not sufficient for the generation of ROS, which suggested that additional TCR signaling was required. Findings from another study (19), as well as from the current study, showed that proximal tyrosine kinases such as Lck and ZAP-70 control the generation of ROS. PKC was also implicated in our study as a necessary mediator of ROS generation. This finding is relevant because Duox1, Duox2, and the other Ca^{2+}-dependent NADPH oxidase, Nox5, are all targets of serine kinases that modulate their activity (34,43). Particularly in the case of Nox5, phosphorylation by PKC at a specific serine residue enhances the sensitivity of this enzyme to activation by lower concentrations of Ca^{2+}. Here, the data indicate that Duox1, but not Duox2, was likely serine-phosphorylated upon TCR stimulation, and the lack of effects of Ca^{2+}-mobilizing compounds, such as thapsigargin or ionomycin, by themselves on the generation of ROS suggests that this modification is required for the activation of Duox1 in T cells. Thus, TCR-induced activation of PKC may phosphorylate Duox1 and promote ROS generation in response to low concentrations of Ca^{2+}.

The current study supports a hypothesis in which Duox1-derived H_2O_2 enhances TCR-proximal signaling events. Knockdown of Duox1 strongly suppressed TCR-stimulated tyrosine phosphorylation of selected targets and weakly inhibited the phosphorylation of TCRζ, but its major effect was on the phosphorylation of Tyr^{319} of ZAP-70. Phosphorylation of Tyr^{319} stabilizes the active state of ZAP-70 (35,40) and provides an adaptor site for the SH2 domains of Lck or PLC-γ1(36,41), so it could be a key regulatory point for TCR-proximal signaling. Cytotoxic T lymphocyte antigen 4 (CTLA-4) is an inhibitory co-receptor on T cells

that dampens T cell responses. One proposed mechanism for its inhibition of TCR signaling is through the decreased phosphorylation of Tyr^{319} of ZAP-70, and the PTPs SHP-2 and SHP-1 seem to be responsible for this effect (44,45). Although ZAP-70, especially Tyr^{319}, is a substrate of Lck, our data suggest that Duox1-mediated regulation of Lck does not play a major role in the decreased phosphorylation of ZAP-70. Phosphorylation of the positive regulatory site in Lck (Tyr^{394}) was not substantially affected by knockdown of Duox1. On the other hand, phosphorylation of the negative regulatory Tyr^{505} residue in Lck was substantially inhibited by knockdown of Duox1, suggesting that Duox1-dependent H_2O_2 limits the activity of Lck by augmenting the phosphorylation of Tyr^{505}. These data suggest that a redox-sensitive target that leads to dephosphorylation of $pTyr^{505}$ in Lck is affected by the activity of Duox1. The PTP CD45 was proposed to directly dephosphorylate $pTyr^{505}$ (46), whereas SHP-2–mediated dephosphorylation of the adaptor protein PAG may inhibit the recruitment of Csk to PAG and the subsequent inhibitory phosphorylation of Lck at Tyr^{505} (9). Both PTPs are redox-sensitive and are inactivated by ROS (24,47). Nevertheless, although some portion of Lck activity may be augmented by the knockdown of Duox1, the overall effects of knockdown of Duox1 on ZAP-70 seem to be dominant in its inhibitory effects on downstream signaling, including on direct ZAP-70 substrates, such as PLC-γ1 and LAT, Ca^{2+} flux, and ERK activation. Griffith *et al*. proposed that signaling through ZAP-70 to ERK activation was redox-sensitive on the basis of the observation that exogenous H_2O_2 did not induce the activation of ERK in the absence of ZAP-70 (48). Thus, our results further support a model in which ZAP-70 serves as a critical oxidant-regulated intermediary between TCR stimulation and downstream signaling.

As discussed earlier, one potential mechanism for the effects of Duox1 on Lck $pTyr^{505}$ and ZAP-70 $pTyr^{319}$ is through redox regulation of SHP-2. Our previous study demonstrated the ROS-mediated phosphorylation of SLP-76–associated proteins, such as Vav1 and ADAP, through TCR-induced oxidation of SHP-2 (24). The current data on the effects of knockdown of Duox1 on the phosphorylation of Vav1 and ADAP support the hypothesis that SHP-2 is a target of Duox1-generated H_2O_2 in T cells. These data are consistent with previous findings that suggest that SHP-2 associates with the adaptor protein Gab2, leading to its membrane localization near the TCR and proximal tyrosine kinases (11). SHP-1 is the other SH2 domain–containing PTP that is proposed to regulate TCR-proximal signaling, but our previous study showed that SHP-1 is not a good target of TCR-induced ROS (24), although it is oxidized upon the stimulation of T cells by antigen-presenting cells (49). Thus, the current data suggest that SHP-2 is recruited to the membrane, where Duox1-dependent H_2O_2 generation is prominent, and that it functions as a redox sensor that regulates proximal and distal TCR signaling events.

Our results further suggest that SHP-2, as a negative regulator, is recruited to a TCR–Lck–ZAP-70 complex through Gab2, and Duox1-mediated enhancement of TCR signaling results from H_2O_2-mediated inactivation of SHP-2. SHP-2 may also be recruited to these proteins in a Gab2-independent manner, but regardless, SHP-2–mediated dephosphorylation of $pTyr^{319}$ of ZAP-70 inhibits the activation of ZAP-70 and its association with Lck, presumably through its SH2 domain. Thus, either siRNA-mediated knockdown of SHP-2 or expression of SHP-2 (C/S) enhanced the formation of the Lck–ZAP-70–TCRζ signaling complex, whereas knockdown of Duox1 inhibited the formation of the complex. Therefore, it seems that SHP-2 can terminate the amplification of an Lck–TCRζ–ZAP-70 feedback loop and that localized production of H_2O_2 by Duox1 inhibits SHP-2–mediated inhibitory effects on this complex.

A previous study of a B cell line suggested a positive feedback loop for Ca^{2+} and ROS in B cell receptor (BCR) signaling but through a very different mechanism (50). Data from that study suggested that the influx of extracellular Ca^{2+} was necessary for the production of ROS and the enhanced activation of the Src family tyrosine kinase Lyn. However, other studies suggested that ROS have a positive role in BCR signaling that is independent of Ca^{2+} (51) or that ROS from Nox2 inhibit the activation of B cells (52). In contrast, our current study on the

role of H_2O_2 in TCR signaling suggests that both phosphorylation and Ca^{2+} released from the ER, not Ca^{2+} influx, contribute to the early TCR-dependent generation of H_2O_2 through the activation of Duox1. The early TCR-induced generation of H_2O_2 seems to inactivate the inhibitor SHP-2 through oxidation of an active-site cysteine, thereby enhancing and sustaining proximal TCR signaling.

Many questions remain, including those about the possible functions of Duox2 in T cells. Our data do not support a role for Duox2 in early TCR-stimulated generation of ROS, regulation of Ca^{2+}, or activation of ERK. NOD2 has an important role in T cells (53), and a study has implicated Duox2 in NOD2-dependent signaling (54), so Duox2 may function more in innate responses by immune cells. Some data suggest that ROS produced by plasma membrane–associated NADPH oxidases leads to the oxidation of intracellular dyes; however, extracellular superoxide dismutase and catalase do not affect TCR-stimulated oxidation of DCFDA in human T blasts or Jurkat cells (fig. S1C) (21), suggesting an intracellular localization of Duox1 in T cells. The association of Duox1 with IP$_3$R1 also supports this conclusion.

The regulation of Ca^{2+} flux by Duox1-derived H_2O_2 could occur at multiple steps in TCR signaling pathways. Our data suggest that enhanced TCR-proximal signaling through a H_2O_2-mediated positive feedback loop leads to augmented release of Ca^{2+} from the ER and the subsequent influx of extracellular Ca^{2+}. Stimulation of the TCR results in co-capping of IP$_3$R1 with the TCR at the sites of TCR engagement, which is where the cellular IP$_3$-generating machinery composed of LAT and PLC-γ1 also accumulates (55). Our results support a model in which Duox1 constitutively associated with IP$_3$R1 in the ER produces H_2O_2 locally near IP$_3$R1-TCR clusters and regulates the tyrosine phosphorylation of proximal kinases. Duox1 may directly regulate the tyrosine phosphorylation of IP$_3$R1, which is important for a sustained Ca^{2+} flux (55). In addition, the ER interacts with different compartments, such as the plasma membrane and mitochondria, through specialized junctions. Thus, Duox1-derived H_2O_2 might also regulate downstream Ca^{2+} mobilization at these sites. Alternatively, Ca^{2+} channels such as the IP$_3$R1, the ryanodine receptor, and the Ca^{2+} release–activated Ca^{2+} (CRAC) channels composed of ORAI1 proteins are redox-sensitive (56–58). The coimmunoprecipitation of Duox1 with IP$_3$R1 suggests that Duox1 may mediate a redox-dependent effect on IP$_3$R1-regulated Ca^{2+} flux.

Therefore, we propose a scheme of TCR-CD3 signal amplification through a positive feedback loop that involves Duox1-mediated production of H_2O_2 (Fig. 10). Upon TCR stimulation, SHP-2 associates with TCR-proximal signaling molecules through Gab2 and inhibits the activation of ZAP-70 through the dephosphorylation of pTyr[319]. Concomitantly, TCR-dependent signal transduction leads to the local production of H_2O_2 through Duox1 and oxidation of the active-site cysteine residue of SHP-2. Duox1-mediated inactivation of SHP-2 thereby diminishes its inhibitory activity and further enhances TCR signaling through the Lck–TCR–ZAP-70 pathway and T cell function.

MATERIALS AND METHODS

Antibodies and reagents

A polyclonal antibody raised against the Arg[618] to His[1044] intracellular fragment of human Duox1 (originally called ThOx1) that recognizes both Duox1 and Duox2 was previously described (42). Antibodies against SHP-2, Grb2, ZAP-70, SHP-1, Vav, and Shc were from Transduction Labs/BD Biosciences. Polyclonal antibodies against Vav, Duox1, SHP-2, Grb2, and SHP-1 were purchased from Santa Cruz Biotechnology. Antibodies against Vav, SLP-76, Gads, Gab2, and phosphotyrosine (4G10); rabbit antibody against IP$_3$R1; and horseradish peroxidase–conjugated rabbit antibody against sheep immunoglobulin G (IgG) were purchased from Upstate Biotechnology. Polyclonal antibody against Duox2 was obtained from Novus.

Monoclonal antibody against pSer (clone 7F12) and the pSer detection set were obtained from Enzo Life Sciences. Antibody against pSer-containing PKC substrates (#2261) was from Cell Signaling Technology. All other chemicals were obtained from Sigma, and all cell culture supplies were from Life Technologies.

Cell culture

Human $CD4^+$ T cells were purified from peripheral blood mononuclear cells by negative selection and activated for 2 days with plate-bound antibody against CD3 (OKT3) and soluble antibody against CD28. T cell blasts were washed and grown for 2 days in complete medium supplemented with recombinant human IL-2 (10 U/ml; Roche Molecular Biochemicals). Jurkat E6-1 cells (American Type Culture Collection) were maintained and propagated as previously described (24). HEK 293 Flp-In clones stably transfected with plasmid expressing hemagglutinin (HA)–tagged Duox1 or HA-tagged Duox2 were generated and maintained as described previously (59).

Plasmid constructs

Mammalian expression vectors that encode HA-tagged wild-type and catalytically inactive SHP-2 [SHP-2 (C/S)] have been previously described (24), as have those that encode wild-type PLC-γ1 and DNPLC-γ1[PLC-γ1 (Y783F)] (32). HA-tagged proteins were immunoprecipitated with the Profound HA-Tag IP/Co-IP kit (Pierce). Mammalian expression vectors encoding untagged and HA-tagged Duox1 have been previously described (59). N17Rac1 was expressed and the NFAT and AP-1 luciferase reporter constructs were used as previously described (26).

Transfection of cells with siRNA or shRNA

To knock down targets with specific siRNAs, we transfected Jurkat cells or activated human $CD4^+$ T cells by electroporation at 250 mV and 950 μF with a GenePulser electroporator (Bio-Rad). The cells were then grown in RPMI 1640 medium with 10% human serum for 40 hours before their use in experiments. To knock down SHP-2, we used 5×10^6 cells per transfection with 0.7 nmol of control siRNA or a total of 0.75 nmol of SHP-2–specific siRNAs. Three different SHP-2–specific siRNAs (5′-GAACATCACGGGCAATTAATT-3′, 5′-GAACACTGGTGATTACTATTT-3′, and 5′-GAAGCACAGTACCGATTTATT-3′; obtained from Dharmacon) were pooled and used to knock down SHP-2. Initial studies compared three Duox1-specific siRNAs: siRNA D2, 5′-GGACTTCCATCGCCTCATT-3′ (D-008126-02, Dharmacon); siRNA J11, 5′-GAGATTCGGCGGAGGTTTG-3′ (J-008126-11, Dharmacon); and siRNA J12, 5′-GCACATCACACGGGCATCA-3′ (D-008126-12, Dharmacon). To knock down Duox1, we used 5×10^6 cells per transfection with 2.1 nmol of Duox1-specific siRNA (5′-GGACTTCCATCGCCTCATT-3′) or 2.1 nmol of control siRNA (ON-TARGETplus siCONTROL Non-Targeting siRNA, D-001810-01, Dharmacon). To knock down Duox1 with shRNA, we used the shRNA plasmid DNA containing the sequence CCGGCCTCATTTCCAAGGATGAGTTCTCGAGAACTCATCCTTGGAAATGAGGTT TTTG (TRCN0000045974, Sigma) and the NT shRNA plasmid (SHC002, Sigma). Jurkat cells transfected by electroporation with 1 μg of either NT shRNA or Duox1-specific shRNA were selected by culturing in the presence of puromycin (1.5 μg/ml) for 3 weeks. Clones were selected and expanded for an additional 2 months and used as stable clones.

Immunoprecipitations and Western blotting

Cell lysis, immunoprecipitations, and Western blotting analysis were performed essentially as previously described (24). Quantitation of bands was preformed by densitometry (Labworks version 4.6, UVP).

Detection of oxidized SHP-2

Jurkat cells were stimulated by cross-linking with antibody against CD3 (OKT3) as described previously (24). The oxidation of SHP-2 was measured as described (39) with some modifications. Cells were fractionated with cytoplasmic extraction buffer followed by membrane extraction buffer (Subcellular Protein Fractionation kit, Thermo Scientific) containing protease inhibitors (Roche) and 50 mM iodoacetamide. SHP-2 was immunoprecipitated from both cytoplasmic and membrane fractions with polyclonal antibodies against SHP-2 (C-18, Santa Cruz Biotechnology). Immunoprecipitated SHP-2 was treated serially with DTT and then pervanadate and analyzed with the affinity-purified oxPTP antibody (R&D Systems) as described previously (39).

Measurement of ROS in Jurkat cells

Kinetic assays of the TCR-stimulated generation of ROS in Jurkat cells measured the oxidation of DCFDA or dihydroethidium (DHE) within limited intervals after the stimulation of cells, essentially as described previously (25). Single endpoint measurements of early-phase generation of ROS in Jurkat cells and human CD4$^+$ T cell blasts were determined by adding DCFDA to the cells before the stimulation of the TCR and measuring the stimulated oxidation of DCFDA over 10- or 15-min time courses, as described previously (26). The stimulated increase in dye oxidation was calculated as the percentage increase in mean channel fluorescence of cells stimulated with antibody against CD3 relative to that of unstimulated cells for each time point with the following equation: $[(MCF_{stim} − MCF_{unstim})/MCF_{unstim}] \times 100$. The oxidation of DCFDA in transiently transfected cells was measured in cells that contained red fluorescent protein (RFP) encoded by a cotransfected plasmid, as previously described (26).

Measurement of Ca^{2+} flux by flow cytometry

Cells (1×10^6/ml) in phosphate-buffered saline were preloaded with Fluo-3 (2 μM) and Fura Red (2 μM) for 30 min in the dark at room temperature in the presence of pluronic and probenecid, as suggested by the supplier (Invitrogen). After washing, cells were resuspended at a density of 2×10^6 cells/ml in phenol red–free complete medium (with extracellular Ca^{2+}) or in Hank's balanced salt solution containing 1% bovine serum albumin (without extracellular Ca^{2+}) and warmed to 37°C. Baseline fluorescence was measured with a FACSCalibur flow cytometer for 30 s before the addition of a soluble stimulus: ionomycin (final concentration, 1 μg/ml) or an IgM against TCR (C305; 1:100 dilution of ascites). Fluorescence signals were collected for an additional 5 min and the data were analyzed with FlowJo software.

RT-PCR analysis

We purified mRNA from cell lysates with poly(dT) magnetic beads (Dynal Biotech) and reverse-transcribed the mRNA with SuperScript II (Invitrogen). PCR products were cloned into the pCRII-TOPO vector (Invitrogen) and sequenced with the M13 F primer. Primer sequences for the genes were as follows: Duox1, 5′-GCAGGACATCAACCCTGCACTCTC-3′ (forward) and 5′-CTGCCATCTACCACACGGATCTGC-3′ (reverse); Duox2, 5′-GCCCTCAACCTAAGCAGCTCACAAC-3′ (forward) and 5′-GAGCACAGTGAGATGCCTGTTCAG-3′ (reverse). The Duox1 PCR product was 532 base pairs (bp) and the Duox2 PCR product was 343 bp.

Measurement of cytokines

TCR-stimulated secretion of cytokines by purified CD4$^+$ T cell blasts was measured by multiplex cytokine bead array kits (Bio-Rad), essentially as previously described (21). The

lower limit of detection of all the cytokines was at 3.2 pg/ml. In this analysis, specimens with individual cytokine amounts that were below the lower limit of detection were arbitrarily assigned to be half of this value (1.6 pg/ml) for that cytokine.

Statistical analysis

Statistical significance was tested with the Wilcoxon signed rank test or the paired Student's *t* test with GraphPad Prism software. Data were considered significantly different when $P < 0.05$.

Supplementary Material

Refer to Web version on PubMed Central for supplementary material.

Acknowledgments

REFERENCES AND NOTES

1. Meng TC, Fukada T, Tonks NK. Reversible oxidation and inactivation of protein tyrosine phosphatases in vivo. Mol. Cell 2002;9:387–399. [PubMed: 11864611]

2. Mahadev K, Zilbering A, Zhu L, Goldstein BJ. Insulin-stimulated hydrogen peroxide reversibly inhibits protein-tyrosine phosphatase 1B in vivo and enhances the early insulin action cascade. J. Biol. Chem 2001;276:21938–21942. [PubMed: 11297536]

3. Ushio-Fukai M, Alexander RW, Akers M, Griendling KK. p38 mitogen-activated protein kinase is a critical component of the redox-sensitive signaling pathways activated by angiotensin II. Role in vascular smooth muscle cell hypertrophy. J. Biol. Chem 1998;273:15022–15029. [PubMed: 9614110]

4. Hehner SP, Breitkreutz R, Shubinsky G, Unsoeld H, Schulze-Osthoff K, Schmitz ML, Dröge W. Enhancement of T cell receptor signaling by a mild oxidative shift in the intracellular thiol pool. J. Immunol 2000;165:4319–4328. [PubMed: 11035067]

5. Cenciarelli C, Wilhelm KG Jr. Guo A, Weissman AM. T cell antigen receptor ubiquitination is a consequence of receptor-mediated tyrosine kinase activation. J. Biol. Chem 1996;271:8709–8713. [PubMed: 8621503]

6. Secrist JP, Burns LA, Karnitz L, Koretzky GA, Abraham RT. Stimulatory effects of the protein tyrosine phosphatase inhibitor, pervanadate, on T-cell activation events. J. Biol. Chem 1993;268:5886–5893. [PubMed: 8383678]

7. Williams MS, Kwon J. T cell receptor stimulation, reactive oxygen species, and cell signaling. Free Radic. Biol. Med 2004;37:1144–1151. [PubMed: 15451054]

8. Singer AL, Koretzky GA. Control of T cell function by positive and negative regulators. Science 2002;296:1639–1640. [PubMed: 12040176]

9. Zhang SQ, Yang W, Kontaridis MI, Bivona TG, Wen G, Araki T, Luo J, Thompson JA, Schraven BL, Philips MR, Neel BG. Shp2 regulates SRC family kinase activity and Ras/Erk activation by controlling Csk recruitment. Mol. Cell 2004;13:341–355. [PubMed: 14967142]

10. Ashwell JD, D'Oro U. CD45 and Src-family kinases: And now for something completely different. Immunol. Today 1999;20:412–416. [PubMed: 10462741]

11. Yamasaki S, Nishida K, Hibi M, Sakuma M, Shiina R, Takeuchi A, Ohnishi H, Hirano T, Saito T. Docking protein Gab2 is phosphorylated by ZAP-70 and negatively regulates T cell receptor signaling by recruitment of inhibitory molecules. J. Biol. Chem 2001;276:45175–45183. [PubMed: 11572860]

12. Plas DR, Johnson R, Pingel JT, Matthews RJ, Dalton M, Roy G, Chan AC, Thomas ML. Direct regulation of ZAP-70 by SHP-1 in T cell antigen receptor signaling. Science 1996;272:1173–1176. [PubMed: 8638162]

13. Chiang GG, Sefton BM. Specific dephosphorylation of the Lck tyrosine protein kinase at Tyr-394 by the SHP-1 protein-tyrosine phosphatase. J. Biol. Chem 2001;276:23173–23178. [PubMed: 11294838]

14. Zhang W, Samelson LE. The role of membrane-associated adaptors in T cell receptor signalling. Semin. Immunol 2000;12:35–41. [PubMed: 10723796]

15. Liu SK, Berry DM, McGlade CJ. The role of Gads in hematopoietic cell signalling. Oncogene 2001;20:6284–6290. [PubMed: 11607830]

16. Oh-hora M, Rao A. Calcium signaling in lymphocytes. Curr. Opin. Immunol 2008;20:250–258. [PubMed: 18515054]

17. Nel AE. T-cell activation through the antigen receptor. Part 1: Signaling components, signaling pathways, and signal integration at the T-cell antigen receptor synapse. J. Allergy Clin. Immunol 2002;109:758–770. [PubMed: 11994696]

18. Jones RG, Bui T, White C, Madesh M, Krawczyk CM, Lindsten T, Hawkins BJ, Kubek S, Frauwirth KA, Wang YL, Conway SJ, Roderick HL, Bootman MD, Shen H, Foskett JK, Thompson CB. The proapoptotic factors Bax and Bak regulate T Cell proliferation through control of endoplasmic reticulum Ca^{2+} homeostasis. Immunity 2007;27:268–280. [PubMed: 17692540]

19. Kaminski M, Kiessling M, Suss D, Krammer PH, Gulow K. Novel role for mitochondria: Protein kinase Cθ-dependent oxidative signaling organelles in activation-induced T-cell death. Mol. Cell. Biol 2007;27:3625–3639. [PubMed: 17339328]

20. Yi JS, Holbrook BC, Michalek RD, Laniewski NG, Grayson JM. Electron transport complex I is required for $CD8^{+}$ T cell function. J. Immunol 2006;177:852–862. [PubMed: 16818739]

21. Jackson SH, Devadas S, Kwon J, Pinto LA, Williams MS. T cells express a Phagocyte-type NADPH oxidase which is activated upon T cell receptor stimulation. Nat. Immunol 2004;5:818–827. [PubMed: 15258578]

22. Los M, Schenk H, Hexel K, Baeuerle PA, Dröge W, Schulze-Osthoff K. IL-2 gene expression and NF-κB activation through CD28 requires reactive oxygen production by 5-lipoxygenase. EMBO J 1995;14:3731–3740. [PubMed: 7641692]

23. Bedard K, Krause KH. The NOX family of ROS-generating NADPH oxidases: Physiology and pathophysiology. Physiol. Rev 2007;87:245–313. [PubMed: 17237347]

24. Kwon J, Qu CK, Maeng JS, Falahati R, Lee C, Williams MS. Receptor-stimulated oxidation of SHP-2 promotes T-cell adhesion through SLP-76-ADAP. EMBO J 2005;24:2331–2341. [PubMed: 15933714]

25. Kwon J, Devadas S, Williams MS. T cell receptor-stimulated generation of hydrogen peroxide inhibits MEK-ERK activation and lck serine phosphorylation. Free Radic. Biol. Med 2003;35:406–417. [PubMed: 12899942]

26. Devadas S, Zaritskaya L, Rhee SG, Oberley L, Williams MS. Discrete generation of superoxide and hydrogen peroxide by T cell receptor stimulation: Selective regulation of mitogen-activated protein kinase activation and Fas ligand expression. J. Exp. Med 2002;195:59–70. [PubMed: 11781366]

27. Ueyama T, Geiszt M, Leto TL. Involvement of Rac1 in activation of multicomponent Nox1- and Nox3-based NADPH oxidases. Mol. Cell. Biol 2006;26:2160–2174. [PubMed: 16507994]

28. Fortemaison N, Miot F, Dumont JE, Dremier S. Regulation of H_2O_2 generation in thyroid cells does not involve Rac1 activation. Eur. J. Endocrinol 2005;152:127–133. [PubMed: 15762196]

29. Hordijk PL. Regulation of NADPH oxidases: The role of Rac proteins. Circ. Res 2006;98:453–462. [PubMed: 16514078]

30. Irvin BJ, Williams BL, Nilson AE, Maynor HO, Abraham RT. Pleiotropic contributions of phospholipase C-γ1(PLC-γ1) to T-cell antigen receptor-mediated signaling: Reconstitution studies of a PLC-γ1-deficient Jurkat T-cell line. Mol. Cell. Biol 2000;20:9149–9161. [PubMed: 11094067]

31. Jayaraman T, Ondriasová E, Ondrias K, Harnick DJ, Marks AR. The inositol 1,4,5-trisphosphate receptor is essential for T-cell receptor signaling. Proc. Natl. Acad. Sci. U.S.A 1995;92:6007–6011. [PubMed: 7597070]

32. Poulin B, Sekiya F, Rhee SG. Intramolecular interaction between phosphorylated tyrosine-783 and the C-terminal Src homology 2 domain activates phospholipase C-γ1. Proc. Natl. Acad. Sci. U.S.A 2005;102:4276–4281. [PubMed: 15764700]

33. Yablonski D, Kadlecek T, Weiss A. Identification of a phospholipase C-γ1 (PLC-γ1) SH3 domain-binding site in SLP-76 required for T-cell receptor-mediated activation of PLC-γ1 and NFAT. Mol. Cell. Biol 2001;21:4208–4218. [PubMed: 11390650]

34. Rigutto S, Hoste C, Grasberger H, Milenkovic M, Communi D, Dumont JE, Corvilain B, Miot F, De Deken X. Activation of dual oxidases Duox1 and Duox2: Differential regulation mediated by camp-dependent protein kinase and protein kinase C-dependent phosphorylation. J. Biol. Chem 2009;284:6725–6734. [PubMed: 19144650]

35. Brdicka T, Kadlecek TA, Roose JP, Pastuszak AW, Weiss A. Intramolecular regulatory switch in ZAP-70: Analogy with receptor tyrosine kinases. Mol. Cell. Biol 2005;25:4924–4933. [PubMed: 15923611]

36. Williams BL, Irvin BJ, Sutor SL, Chini CC, Yacyshyn E, Bubeck Wardenburg J, Dalton M, Chan AC, Abraham RT. Phosphorylation of Tyr319 in ZAP-70 is required for T-cell antigen receptor-dependent phospholipase C-γ1 and Ras activation. EMBO J 1999;18:1832–1844. [PubMed: 10202147]

37. Aghazadeh B, Lowry WE, Huang XY, Rosen MK. Structural basis for relief of autoinhibition of the Dbl homology domain of proto-oncogene Vav by tyrosine phosphorylation. Cell 2000;102:625–633. [PubMed: 11007481]

38. Yamasaki S, Nishida K, Sakuma M, Berry D, McGlade CJ, Hirano T, Saito T. Gads/Grb2-mediated association with LAT is critical for the inhibitory function of Gab2 in T cells. Mol. Cell. Biol 2003;23:2515–2529. [PubMed: 12640133]

39. Persson C, Kappert K, Engström U, Ostman A, Sjöblom T. An antibody-based method for monitoring in vivo oxidation of protein tyrosine phosphatases. Methods 2005;35:37–43. [PubMed: 15588984]

40. Deindl S, Kadlecek TA, Brdicka T, Cao X, Weiss A, Kuriyan J. Structural basis for the inhibition of tyrosine kinase activity of ZAP-70. Cell 2007;129:735–746. [PubMed: 17512407]

41. Pelosi M, Di Bartolo V, Mounier V, Mège D, Pascussi JM, Dufour E, Blondel A, Acuto O. Tyrosine 319 in the interdomain B of ZAP-70 is a binding site for the Src homology 2 domain of Lck. J. Biol. Chem 1999;274:14229–14237. [PubMed: 10318843]

42. De Deken X, Wang D, Many MC, Costagliola S, Libert F, Vassart G, Dumont JE, Miot F. Cloning of two human thyroid cDNAs encoding new members of the NADPH oxidase family. J. Biol. Chem 2000;275:23227–23233. [PubMed: 10806195]

43. Jagnandan D, Church JE, Banfi B, Stuehr DJ, Marrero MB, Fulton DJ. Novel mechanism of activation of NADPH oxidase 5. Calcium sensitization via phosphorylation. J. Biol. Chem 2007;282:6494–6507. [PubMed: 17164239]

44. Guntermann C, Alexander DR. CTLA-4 suppresses proximal TCR signaling in resting human CD4$^+$ T cells by inhibiting ZAP-70 Tyr^{319} phosphorylation: A potential role for tyrosine phosphatases. J. Immunol 2002;168:4420–4429. [PubMed: 11970985]

45. Lee KM, Chuang E, Griffin M, Khattri R, Hong DK, Zhang W, Straus D, Samelson LE, Thompson CB, Bluestone JA. Molecular basis of T cell inactivation by CTLA-4. Science 1998;282:2263–2266. [PubMed: 9856951]

46. Mustelin T, Coggeshall KM, Altman A. Rapid activation of the T-cell tyrosine protein kinase pp56^{lck} by the CD45 phosphotyrosine phosphatase. Proc. Natl. Acad. Sci. U.S.A 1989;86:6302–6306. [PubMed: 2548204]

47. Takakura K, Beckman JS, MacMillan-Crow LA, Crow JP. Rapid and irreversible inactivation of protein tyrosine phosphatases PTP1B, CD45, and LAR by peroxynitrite. Arch. Biochem. Biophys 1999;369:197–207. [PubMed: 10486138]

48. Griffith CE, Zhang W, Wange RL. ZAP-70-dependent and -independent activation of Erk in Jurkat T cells. Differences in signaling induced by H_2O_2 and Cd3 cross-linking. J. Biol. Chem 1998;273:10771–10776. [PubMed: 9553143]

49. Schnell FJ, Alberts-Grill N, Evavold BD. CD8$^+$ T cell responses to a viral escape mutant epitope: Active suppression via altered SHP-1 activity. J. Immunol 2009;182:1829–1835. [PubMed: 19201834]

50. Singh DK, Kumar D, Siddiqui Z, Basu SK, Kumar V, Rao KV. The strength of receptor signaling is centrally controlled through a cooperative loop between Ca^{2+} and an oxidant signal. Cell 2005;121:281–293. [PubMed: 15851034]

51. Capasso M, Bhamrah MK, Henley T, Boyd RS, Langlais C, Cain K, Dinsdale D, Pulford K, Khan M, Musset B, Cherny VV, Morgan D, Gascoyne RD, Vigorito E, Decoursey TE, Maclennan IC, Dyer MJ. HVCN1 modulates BCR signal strength via regulation of BCR-dependent generation of reactive oxygen species. Nat. Immunol 2010;11:265–272. [PubMed: 20139987]

52. Richards SM, Clark EA. BCR-induced superoxide negatively regulates B-cell proliferation and T-cell-independent type 2 Ab responses. Eur. J. Immunol 2009;39:3395–3403. [PubMed: 19877015]

53. Shaw MH, Reimer T, Sanchez-Valdepenas C, Warner N, Kim YG, Fresno M, Nunez G. T cell–intrinsic role of Nod2 in promoting type 1 immunity to *Toxoplasma gondii*. Nat. Immunol 2009;10:1267–1274. [PubMed: 19881508]

54. Lipinski S, Till A, Sina C, Arlt A, Grasberger H, Schreiber S, Rosenstiel P. DUOX2-derived reactive oxygen species are effectors of NOD2-mediated antibacterial responses. J. Cell Sci 2009;122:3522–3530. [PubMed: 19759286]

55. deSouza N, Cui J, Dura M, McDonald TV, Marks AR. A function for tyrosine phosphorylation of type 1 inositol 1,4,5-trisphosphate receptor in lymphocyte activation. J. Cell Biol 2007;179:923–934. [PubMed: 18056410]

56. Aracena-Parks P, Goonasekera SA, Gilman CP, Dirksen RT, Hidalgo C, Hamilton SL. Identification of cysteines involved in S-nitrosylation, S-glutathionylation, and oxidation to disulfides in ryanodine receptor type 1. J. Biol. Chem 2006;281:40354–40368. [PubMed: 17071618]

57. Bogeski I, Kummerow C, Al-Ansary D, Schwarz EC, Koehler R, Kozai D, Takahashi N, Peinelt C, Griesemer D, Bozem M, Mori Y, Hoth M, Niemeyer BA. Differential redox regulation of ORAI ion channels: A mechanism to tune cellular calcium signaling. Sci. Signal 2010;3:ra24. [PubMed: 20354224]

58. Redondo PC, Salido GM, Rosado JA, Pariente JA. Effect of hydrogen peroxide on Ca^{2+} mobilisation in human platelets through sulphydryl oxidation dependent and independent mechanisms. Biochem. Pharmacol 2004;67:491–502. [PubMed: 15037201]

59. Morand S, Ueyama T, Tsujibe S, Saito N, Korzeniowska A, Leto TL. Duox maturation factors form cell surface complexes with Duox affecting the specificity of reactive oxygen species generation. FASEB J 2009;23:1205–1218. [PubMed: 19074510]
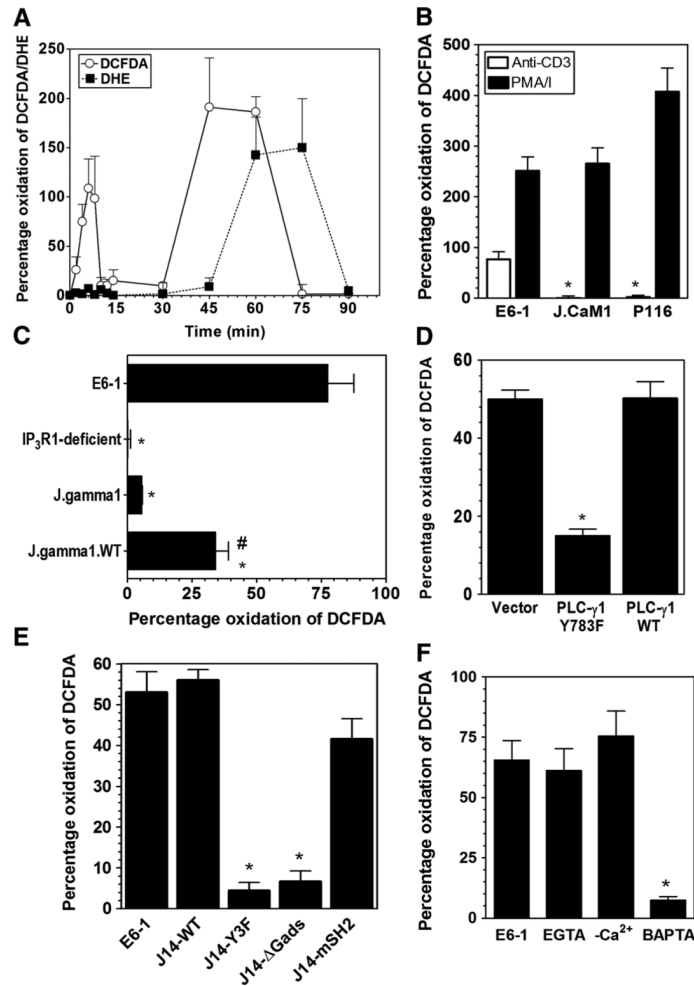
Fig. 1.
Signaling pathways that regulate the early-phase generation of ROS in TCR-stimulated Jurkat cells. (**A**) Kinetics of TCR-induced generation of ROS in Jurkat cells detected within the indicated intervals by measurement of the oxidation of DCFDA (open circles) or DHE (solid squares). (**B**) TCR-induced oxidation of DCFDA measured in 10-min endpoint assays after stimulation with antibody against CD3 in control Jurkat cells (E6-1) or in Jurkat cell clones in which Lck (J.CaM1) or ZAP-70 (P116) is absent. Cells were stimulated by antibody against CD3 (OKT3) cross-linked by secondary antibodies (open bars) or with PMA (10 ng/ml) and ionomycin (1 μg/ml; solid bars). (**C**) TCR-induced oxidation of DCFDA in wild-type (WT) Jurkat cells (E6-1), in clones that are deficient in IP_3R1 (IP_3R1-deficient) or PLC-γ1 (J.gamma1), or in a PLC-γ1–deficient clone that was reconstituted with PLC-γ1 (J.gamma1.WT). *$P < 0.05$, when compared to Jurkat E6-1 cells; #$P < 0.05$, when compared to J.gamma1 cells. (**D**) TCR-induced oxidation of DCFDA in Jurkat cells that were transiently transfected with empty vector or with plasmids encoding either WT PLC-γ1 or the Y783F mutant PLC-γ1 in the presence of a plasmid encoding RFP. The data represent the percentage of TCR-stimulated oxidation of DCFDA in RFP^{+} cells. (**E**) TCR-induced oxidation of DCFDA in WT Jurkat cells or in SLP-76–deficient clones (J14) that were stably transfected with plasmids encoding full-length SLP-76 (J14-WT), a tyrosine mutant of SLP-76 (J14-Y3F), an SLP-76 mutant in which the proline-rich domain was deleted (J14-ΔGads), or a variant SLP-76 in which the SH2 domain is mutated (J14-mSH2). (**F**) TCR-induced oxidation of DCFDA in WT Jurkat cells in the presence or absence of the Ca^{2+} chelators EGTA and BAPTA or in cells

stimulated in buffer lacking Ca^{2+} ($-Ca^{2+}$). In all of the panels, the data represent means $\pm$ SEM of at least four separate experiments. *$P < 0.05$.
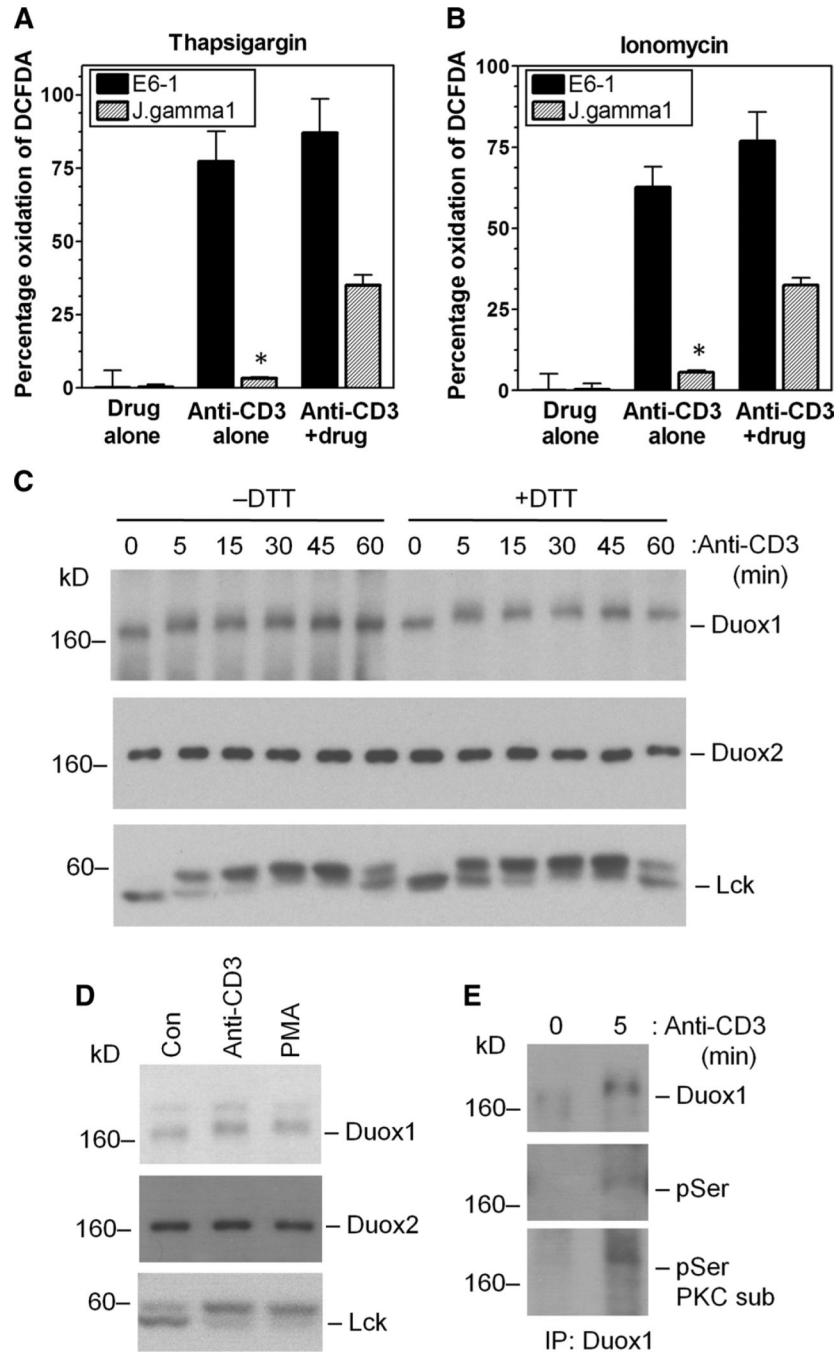
Fig. 2.
Activation of the NADPH oxidase Duox1 in TCR-stimulated Jurkat cells. (**A** and **B**) Ca^{2+}-mobilizing agents alone do not trigger the early-phase generation of ROS. TCR-induced oxidation of DCFDA was measured 10 min after TCR stimulation of Jurkat E6-1 cells or PLC-γ1–deficient Jurkat cells (J.gamma1) incubated with either (A) thapsigargin or (B) ionomycin. The data represent the mean ± SEM of five separate experiments. *$P < 0.05$.(**C** and **D**) TCR-induced posttranslational modification of Duox1 in Jurkat cells. Western blotting analysis of (C) TCR- or (D) PMA-induced changes in the electrophoretic mobility of Duox1, Duox2, or Lck protein from cell lysates prepared in the presence (+) or absence (−) of DTT. Con, control, unstimulated cells. (**E**) Detection of the phosphorylation of Duox1 in response to TCR

stimulation. Duox1 was immunoprecipitated (IP) and analyzed by Western blotting with (from top) antibodies against Duox1, pSer, or pSer-containing PKC substrates (PKC sub).
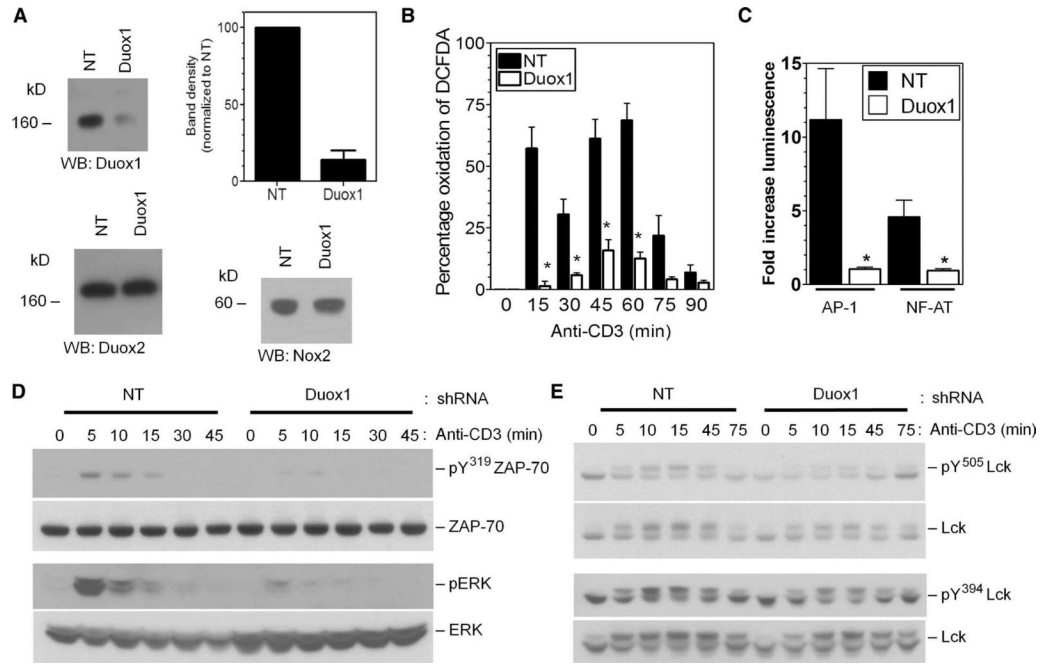
Fig. 3.
Effects of the knockdown of Duox1 on TCR signaling in Jurkat cells. (**A**) Analysis of the abundances of Duox1, Duox2, and Nox2 proteins in Jurkat cell clones expressing NT or Duox1-specific (Duox1) shRNAs. The graph represents the average band density of Duox1 normalized to that in NT cells from three separate blots. *$P < 0.05$. WB, Western blotting. (**B**) Kinetics of TCR-induced oxidation of DCFDA in Jurkat cells stably transfected with NT (closed bars) or Duox1-specific (open bars) shRNA-expressing vectors. *$P < 0.05$. (**C**) TCR-induced activation of luciferase reporter plasmids driven by consensus sequences for AP-1 or NFAT in Jurkat cell clones expressing NT or Duox1-specific shRNAs. The data represent the mean fold increase in the amount of luciferase signal relative to that of unstimulated controls ± SEM from five experiments. *$P < 0.05$. (**D** and **E**) The kinetics of TCR-induced phosphorylation of ZAP-70 (Y319), ERK1 and ERK2, and Lck (Y394 and Y505) were determined by Western blotting analysis of whole-cell lysates from stable Jurkat clones expressing NT or Duox1-specific shRNAs with phosphospecific antibodies. Blots were then stripped and analyzed for total ZAP-70, ERK1 and ERK2, and Lck content to control for loading and to determine the effects of shRNAs.
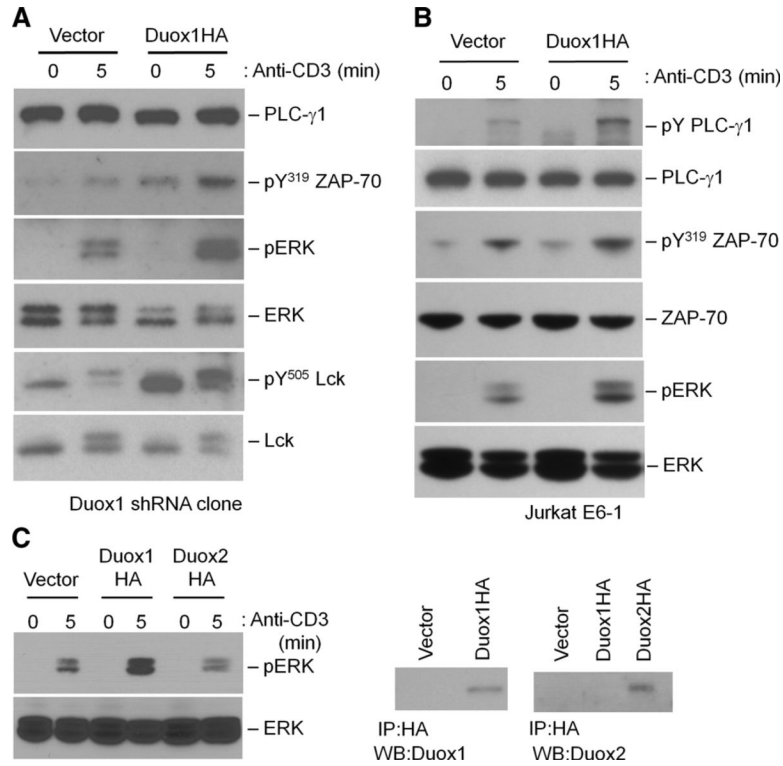
Fig. 4.
Effects of the increased abundance of Duox1 on TCR signaling in Jurkat cells. (**A**) The Duox1-knockdown Jurkat cell clone was transfected with an empty vector or with a plasmid encoding HA-tagged Duox1. TCR-induced phosphorylation of ZAP-70 (Y319), ERK1 and ERK2, and Lck (Y394 and Y505) was detected after 5 min of stimulation by Western blotting analysis of whole-cell lysates with phosphospecific antibodies. Blots were then stripped and analyzed for total PLC-γ1, ERK1 and ERK2, and Lck content to control for loading and to determine the effects of the increased abundance of Duox1. (**B**) Jurkat cells were transiently transfected with an empty vector or with a plasmid encoding HA-tagged Duox1. TCR-induced phosphorylation of PLC-γ1, ZAP-70 (Y319), and ERK1 and ERK2 was analyzed as described for (A). Blots were then stripped and analyzed for total PLC-γ1, ZAP-70, and γ-tubulin content to control for loading. (**C**) Activation of ERK1 and ERK2 was measured in Jurkat cells transiently transfected with empty vector, plasmid encoding HA-tagged Duox1, or plasmid encoding HA-tagged Duox2. HA-tagged proteins were immunoprecipitated from their respective lysates and analyzed by Western blotting with antibodies against Duox1 or Duox2.
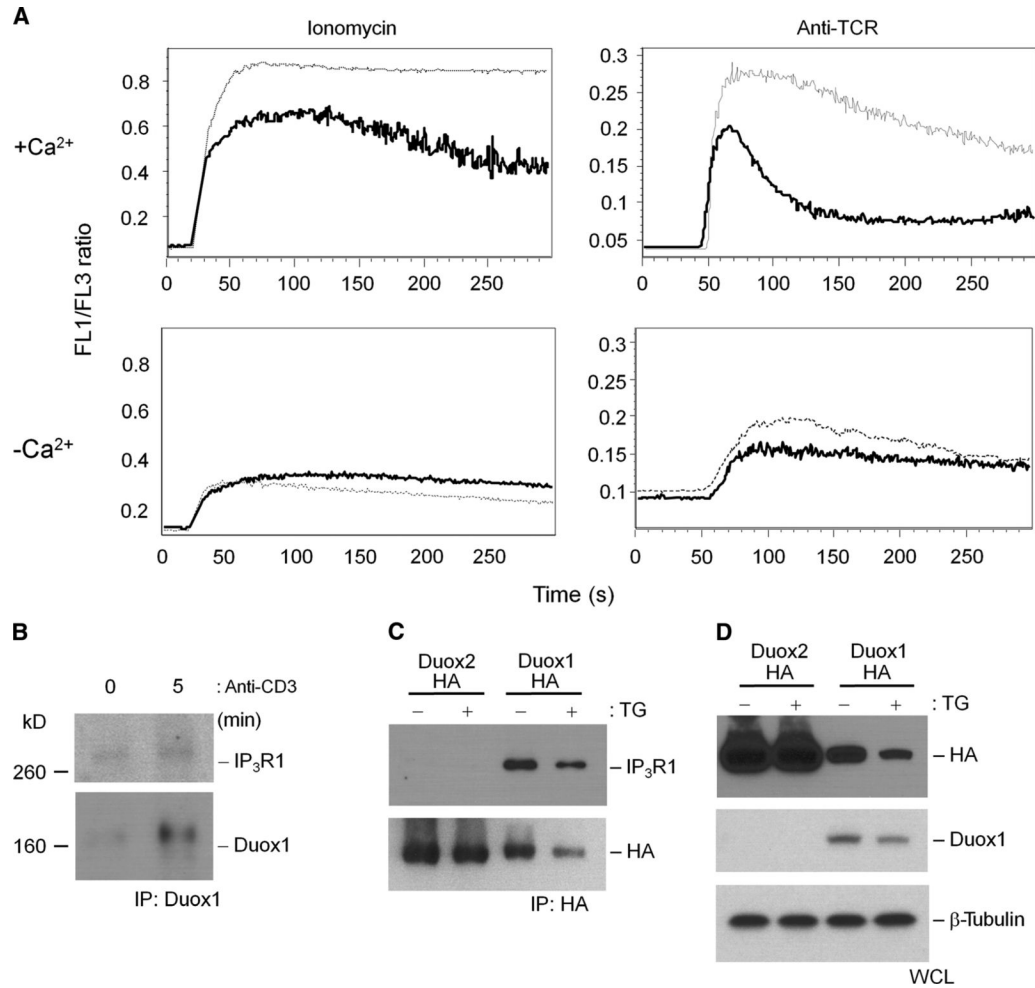
Fig. 5.
Duox1-mediated regulation of intracellular Ca^{2+}. (**A**) TCR-induced Ca^{2+} flux in Jurkat cell clones stably transfected with NT (dotted lines) or Duox1-specific (solid lines) shRNAs. Cells were loaded with Fluo-3 and Fura Red, stimulated with ionomycin or soluble IgM against TCR in the presence ($+Ca^{2+}$) or absence ($-Ca^{2+}$) of extracellular Ca^{2+}, and immediately analyzed by flow cytometry. The data are presented as the ratio of Fluo-3 to Fura Red fluorescence over time and are representative of five separate experiments. (**B**) Association of IP_3R1 with Duox1 in Jurkat cells. Duox1 was immuno-precipitated from lysates of Jurkat cells that were unstimulated or stimulated by TCR cross-linking for 5 min, and immunoprecipitates were analyzed by Western blotting for the presence of IP_3R1 or Duox1. (**C**) IP_3R1 coimmunoprecipitates with Duox1, but not Duox2, in stably transfected HEK 293 cells. Flp-In 293 clones stably expressing HA-tagged Duox1 or HA-tagged Duox2 were generated and incubated in the presence or absence of thapsigargin (TG). HA-tagged proteins were immunoprecipitated from the respective cell lysates and analyzed by Western blotting with antibodies against IP_3R1 or the HA tag. (**D**) Whole-cell lysates (WCL) from the stable clones were analyzed by Western blotting for the presence of HA, Duox1, and β-tubulin as loading controls.
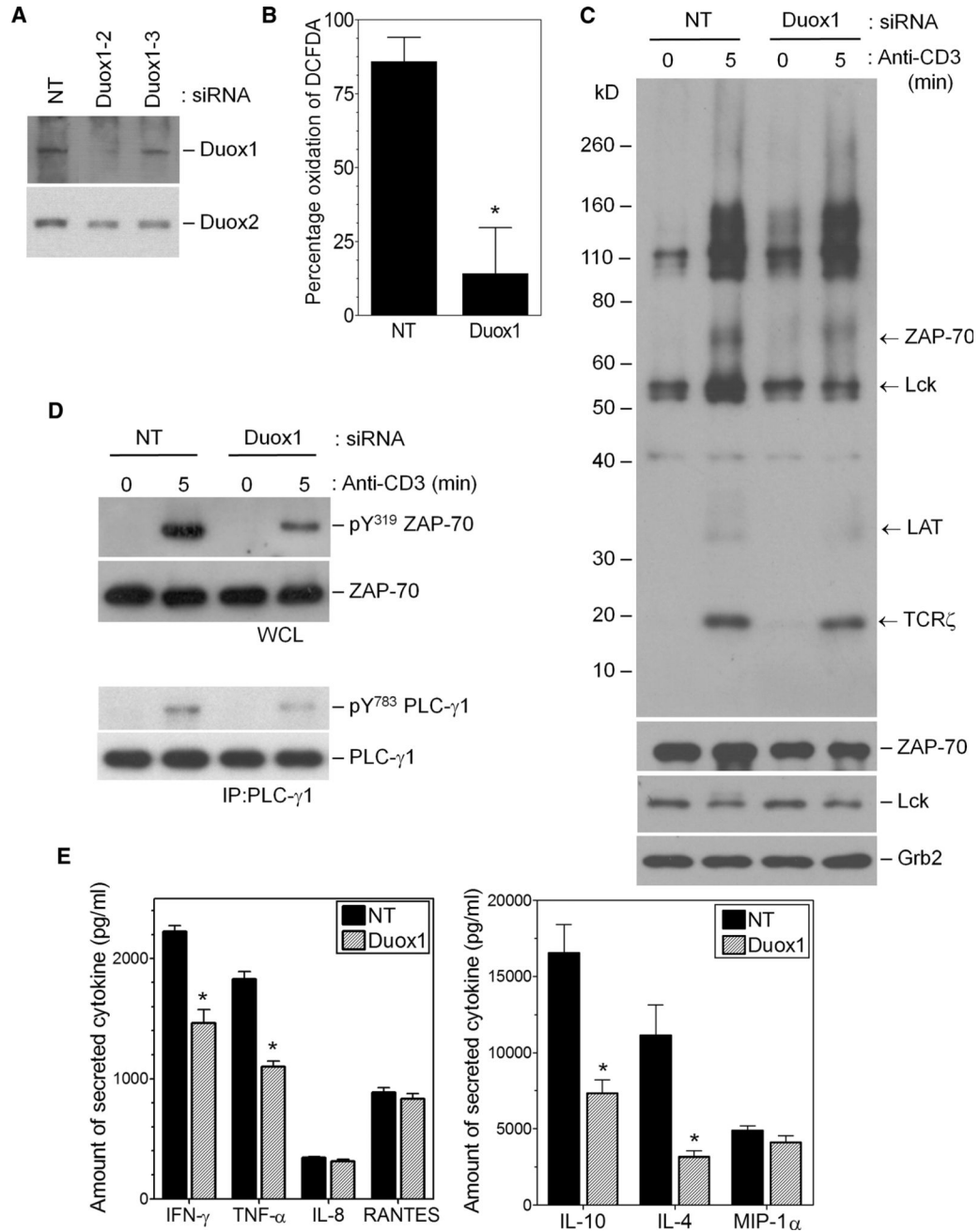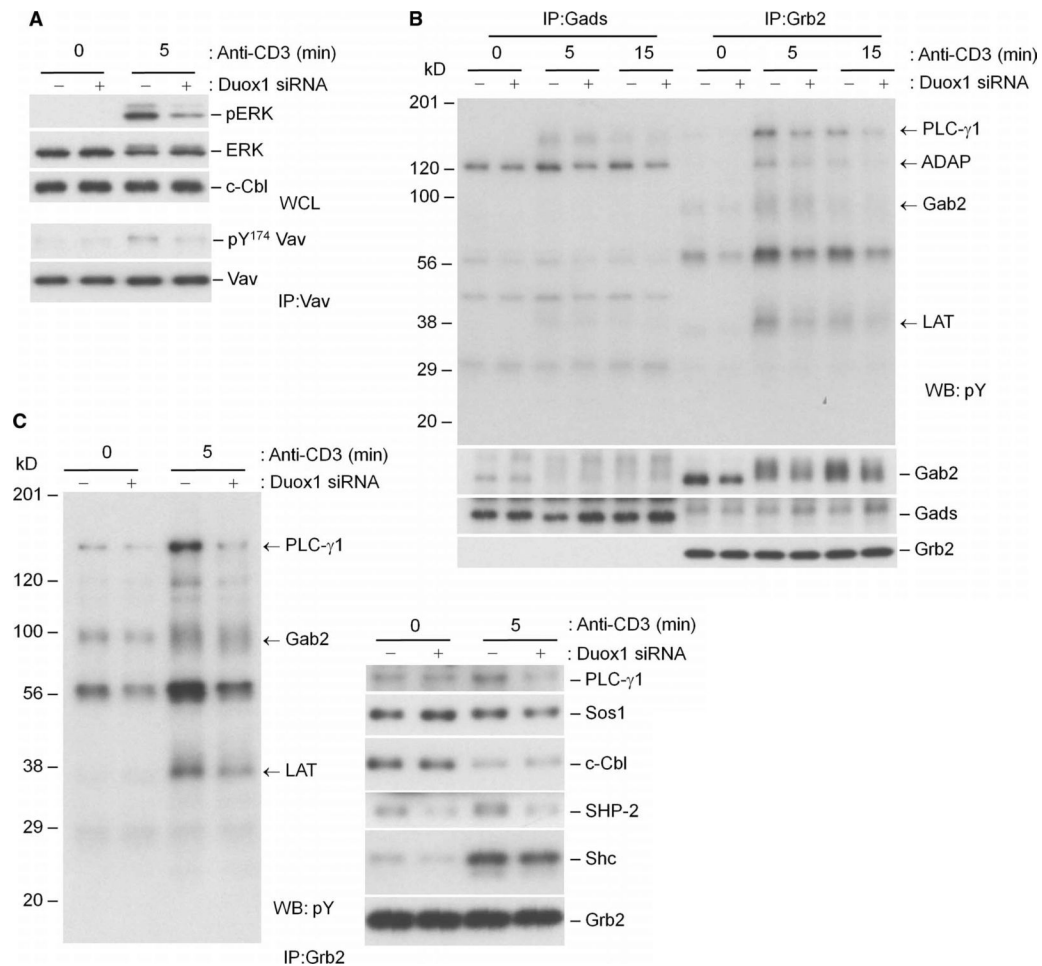
Fig. 6.
Effects of knockdown of Duox1 on TCR signaling in CD4^{+} human T cell blasts. CD4^{+} human T cell blasts were transfected with NT or Duox1-specific siRNAs and cultured for 40 hours. (**A**) Effects of NT or different Duox1-specific siRNAs (Duox1-2 or Duox1-3) on the abundances of Duox1 and Duox2 proteins. (**B**) Effects of NT or Duox1-specific siRNAs on TCR-induced oxidation of DCFDA. The data represent the mean ± SEM of four separate experiments. *$P < 0.05$. (**C** and **D**) Western blotting analysis was performed on post-nuclear cell lysates for the presence of (C) tyrosine phosphorylation, with an antibody against phosphotyrosine (pY) residues, or (D) phosphorylation of ZAP-70 (Y319) in cells stimulated for 5 min by TCR cross-linking. (D) PLC-γ1 was immunoprecipitated from the respective cell lysates and analyzed by Western blotting with a phosphospecific (Y783) antibody. Western

blots were then stripped and analyzed for the presence of ZAP-70, Lck, Grb2, and PLC-γ1 as loading and siRNA controls. (**E**) Effects of knockdown of Duox1 on cytokine production. Cells transfected with the siRNAs described in (A) were stimulated for 8 hours with plate-bound OKT3, and supernatants were analyzed by multiplex bead arrays for the secretion of the indicated cytokines. The data represent the mean ± SEM of duplicate wells from three separate experiments. *$P < 0.05$.

Fig. 7.
Effects of knockdown of Duox1 on TCR-stimulated activation of ERK and signaling phosphoproteins associated with the adaptor proteins Gads and Grb2. CD4^{+} human T cell blasts were transfected with NT or Duox1-specific siRNAs as described for Fig. 6. (**A**) TCR-induced phosphorylation of ERK1 and ERK2 was analyzed after 5 min of stimulation by Western blotting of whole-cell lysates with phosphospecific antibodies. Vav1 was immunoprecipitated from the respective cell lysates and analyzed by Western blotting with a phosphospecific (Y174) antibody. Blots were then stripped and analyzed for total Vav1, Lck, and c-Cbl content to control for loading. (**B**) Gab2 is primarily associated with Grb2 in human T cells, and tyrosine phosphorylation of Grb2-associated proteins is decreased by knockdown of Duox1. CD4^{+} human T cell blasts were transfected with NT or Duox1-specific siRNAs and stimulated by TCR cross-linking as described for Fig. 6. Gads and Grb2 were serially immunoprecipitated from precleared lysates, and protein phosphorylation was detected by Western blotting analysis with an antibody against phosphotyrosine. The blot was then stripped and analyzed with antibodies against Gab2, Gads, and Grb2. (**C**) Tyrosine phosphorylation of Grb2-associated proteins is decreased by knockdown of Duox1. Samples immunoprecipitated with antibody against Grb2 were analyzed by Western blotting with an antibody against phosphotyrosine and with other antibodies specific for the coimmunoprecipitated proteins.
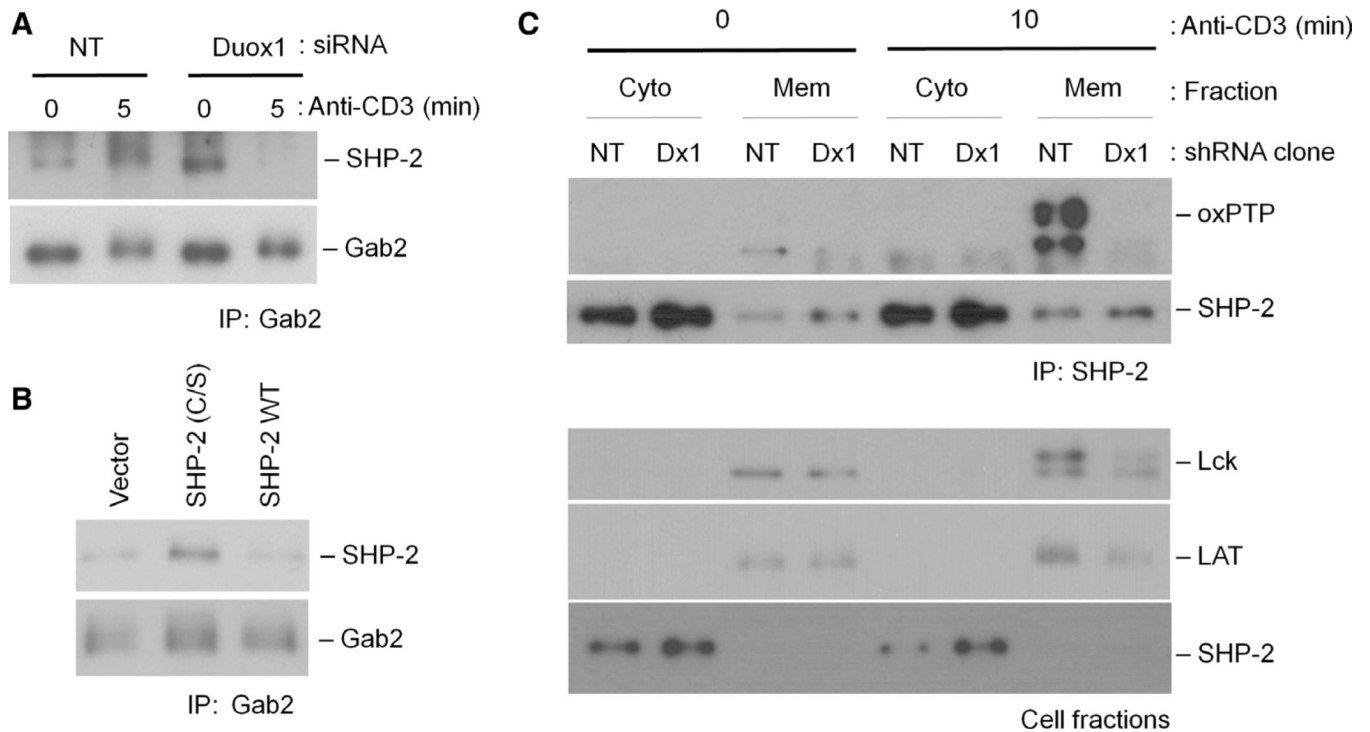
Fig. 8.
Duox1-mediated redox regulation of SHP-2. (**A** and **B**) Duox1-mediated regulation of the interaction between SHP-2 and Gab2. (A) CD4^{+} human T cell blasts were transfected with NT or Duox1-specific siRNAs and stimulated by cross-linking of the TCR, as described for Fig. 6. The presence of SHP-2 in Gab2 antibody samples immunoprecipitated with antibody against Gab2 was detected by Western blotting with antibody against SHP-2. As a control for loading, Gab2 was detected by specific antibody. (B) Jurkat cells were transfected with empty vector, plasmid encoding an active-site cysteine mutant of SHP-2 [SHP-2 (C/S)], or plasmid encoding WT SHP-2 (SHP-2 WT) and stimulated by TCR cross-linking. The presence of SHP-2 in samples immunoprecipitated with antibody against Gab2 was detected by Western blotting with antibody against SHP-2. As a loading control, Gab2 was detected with a Gab2-specific antibody. (**C**) Effects of knockdown of Duox1 on the oxidation of SHP-2. TCR-stimulated oxidation of SHP-2 was detected in Jurkat clones expressing plasmids encoding NT or Duox1-specific shRNAs after TCR cross-linking. Cells were fractionated into cytoplasmic (Cyto) and membrane (Mem) fractions, and SHP-2 was immunoprecipitated from both fractions. Immunoprecipitates were analyzed by Western blotting with the oxPTP antibody to detect oxidation of the active-site cysteine of SHP-2. Ly-sates of cellular fractions were analyzed by Western blotting for the presence of Lck, LAT, and SHP-2 to control for subcellular separation and loading.
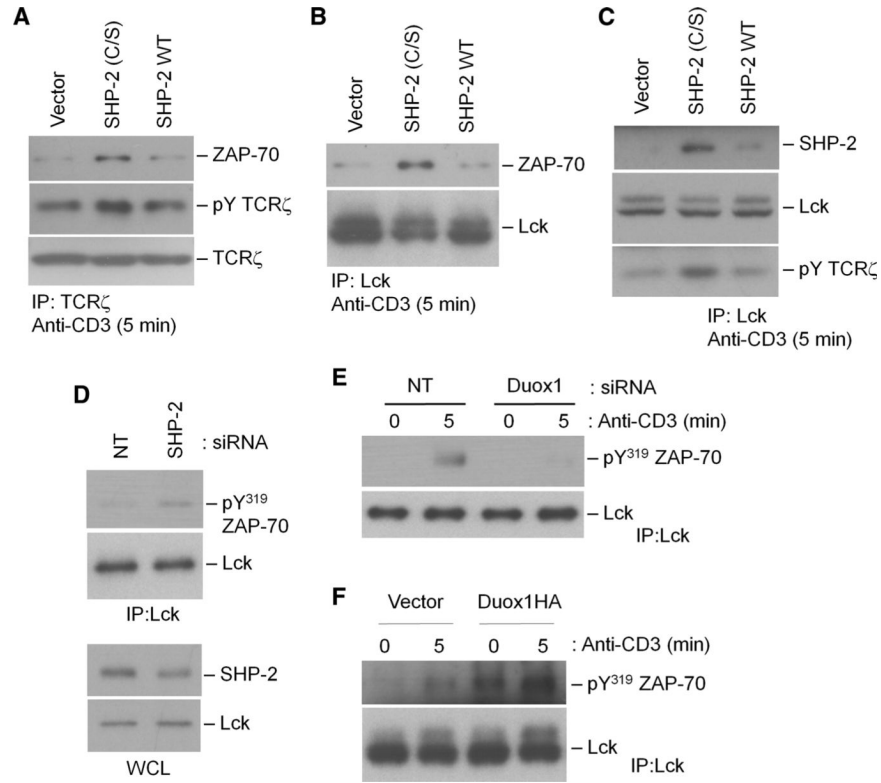
Fig. 9.
SHP-2–mediated regulation of the interaction among Lck, TCR, and ZAP-70. (**A** to **C**) Jurkat cells were transfected with empty vector, plasmid encoding SHP-2 (C/S), or plasmid encoding WT SHP-2 and stimulated by TCR cross-linking for 5 min as described for Fig. 3. TCRζ (A) or Lck (B and C) was immunoprecipitated from precleared lysates, and immunoprecipitates were analyzed by Western blotting with antibodies against ZAP-70, TCRζ, Lck, or SHP-2 or with antibody against phosphotyrosine to detect tyrosine phosphorylation of the TCRζ chain. (**D**) Human CD4^{+} T cell blasts were transfected with NT or SHP-2–specific siRNAs and stimulated by TCR cross-linking for 5 min. Post-nuclear cell lysates were analyzed by Western blotting with an antibody against SHP-2. Lck was immunoprecipitated and samples were analyzed by Western blotting with an antibody against pY319 ZAP-70. (**E**) CD4^{+} human T cell blasts were transfected with NT or Duox1-specific siRNAs and stimulated by TCR cross-linking as described for Fig. 6. Lck was immunoprecipitated from precleared lysates, and samples were analyzed by Western blotting with an antibody against pY319 ZAP-70. (**F**) Jurkat cells were transiently transfected with empty vector or with plasmid encoding HA-tagged Duox1, and cells were stimulated by TCR cross-linking as described for Fig. 3. Lck was immunoprecipitated from pre-cleared lysates, and samples were analyzed by Western blotting with an antibody against pY319 ZAP-70.
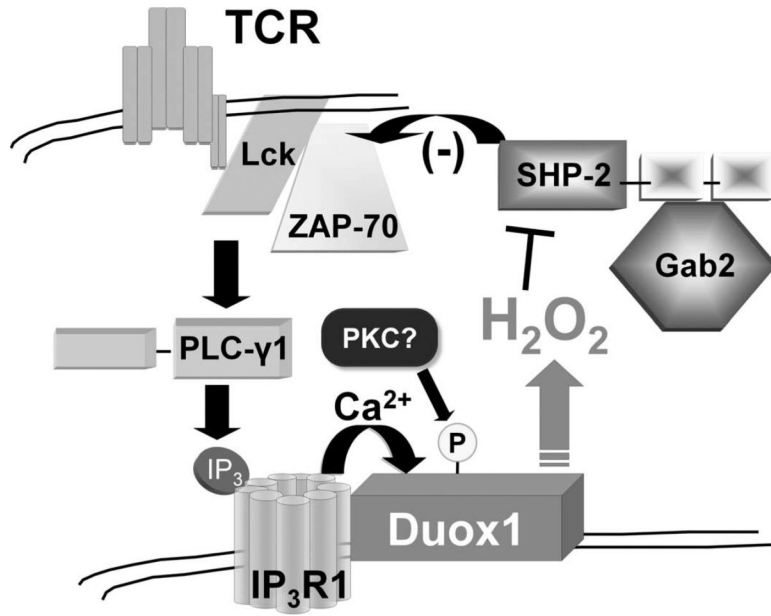
Fig. 10.
Proposed model for the Duox1-mediated regulation of TCR signaling. TCR stimulation leads, through the activation of several protein kinases, to the activation of PLC-γ1. The resulting hydrolysis of phosphatidylinositol-4,5-bisphosphate to diacylglycerol and IP_3 leads to the binding of IP_3 to IP_3R1, which causes the release of Ca^{2+} from the ER. Duox1 that is associated with IP_3R1 is activated by the Ca^{2+} that is released from ER and also through phosphorylation, potentially by PKC. Duox1-mediated production of ROS inactivates the SHP-2 protein that is associated with Gab2 in proximity to complexes of TCR, Lck, and ZAP-70. Oxidative inactivation of SHP-2 relieves the inhibitory effects of SHP-2 activity on ZAP-70 and promotes further TCR signaling, such as the activation of ERK and the influx of extracellular Ca^{2+}.